International Journal of Dynamics and Control (2019) 7:226–240
https://doi.org/10.1007/s40435-018-0437-8

Exogenous input and state estimation for a class of nonlinear dynamic systems in the presence of the unknown but bounded disturbances

M. A. Alirezapouri[1] · A. R. Vali[1] · H. Khaloozadeh[2] · M. R. Arvan[1]

Received: 12 January 2018 / Revised: 13 April 2018 / Accepted: 27 April 2018 / Published online: 15 May 2018

Abstract

Estimation of the exogenous input is an important topic in various applications. Unknown inputs can dramatically degrade the estimation performance in systems with unknown but bounded (UBB) disturbances. In this study, based on UBB assumption of the input and observation disturbances, a method is proposed for simultaneous estimation of the unknown input, state vector, and disturbance for a class of nonlinear dynamical systems. Based on the affine transformation of convex sets, disturbance and unknown input are considered as new state variables and therefore the nonlinear system of state equations is rearranged. Based on interval mathematics, the linearization error of the process and observation equations are bounded with convex closed sets and then combined with the ellipsoidal sets that representing system disturbance. The augmented state vector is estimated based on extended set value observer. To satisfy the stability of the proposed method, the input to state stability and boundedness of the estimation error is analyzed. The proposed method performance is verified by various numerical simulations and compared with other input estimation methods. Numerical simulations show the acceptable performance of the proposed algorithm in the simultaneously estimation of the unknown input, disturbance, and state vector rather than other unknown input estimation method.

Keywords Input estimation · Nonlinear filtering · UBB uncertainty

1 Introduction

The state vector estimation of uncertain nonlinear dynamic systems has attracted considerable attention in the control and signal processing applications [1]. Systematic modeling errors, noise in the observations or measurements, and input disturbances are the main sources of uncertainty in uncertain dynamical systems. Different methods of state estimation can be obtained using various approaches of uncertainty modeling. Among the different proposed estimators, the Kalman filters are developed and had used in various applications [2]. In Kalman filtering theory, the system uncertainty is modeled based on stochastic approach [3]. H_∞ filtering is another approach for state estimation [4]. In H_∞ filtering, the uncertainties are assumed unknown signals with bounded [4]. These filters are usually robust in the presence of dynamic system uncertainties.

Another approach to uncertainty modeling and filtering is unknown but bounded (UBB) approach [5]. In this approach, the uncertainties are considered unknown except that they belong to given convex closed sets [5–7]. The UBB approach-based estimation leads to a feasible set of state vector where it is persistent respect to the dynamic system model and the disturbance bounds. In UBB based filters, usually, the center of the estimated set is used as estimated vector based on the "minimum of maximum estimation error" criteria [7]. The UBB filters are identified by various names such as UBB-based filter, set value observer (SVO), set membership filter (SMF), and set value Kalman filter. Schweppe in [5] used an ellipsoidal approximation algorithm with computational advantages. In this algorithm, the initial state, input disturbances and observation error are modeled by ellipsoidal sets, and the observations are then used for bounding the ellipsoidal set on the predicted set. Due to the proper mathematical form and the lower computational burden, UBB based algorithms that use ellipsoidal set outer-bounding concept, have

✉ M. A. Alirezapouri
Maa_Pouri@mut.ac.ir

1 Faculty of Electrical and Computer Engineering, Malek-Ashtar University of Technology, Tehran, Iran

2 Departments of System and Control, Faculty of Electrical Engineering, K. N. Toosi University of Technology, Tehran, Iran

been attracted and developed rather than other UBB based filters. In contrast to ellipsoidal bounding algorithms, using other convex sets for uncertainty modeling requires considerable computational resources. Owing to advances in the computational ability of modern digital processors, it has become possible to use other sets in UBB-approach-based state estimation. Zonotopes [8], parallelotopes [9], and triangulations [10] are some sets that are used for uncertainty modeling. Several studies have been conducted to address the limitations of the basic ellipsoidal outer bounding filter, such as computation burden, numerical instability, non-optimal ellipsoidal bounding, and using SVOs for nonlinear systems. For example, Maksarov and Norton [11] had established the optimal ellipsoidal state-bounding algorithm, Gollamudi et al. [12] has proposed a set value observer that use optimal bounding ellipsoidal sets with a selective observation update strategy, an extended set-membership filter (ESMF) where using interval analysis have developed by Schulte and Campbell [13], Wei et al. [14] proposed a SVO based on semi-definite programming with constrained error. In [15] a method for reducing the computation load for linear systems was proposed.

Generally, in the state estimation problems, the control input vector is usually considered to be well-known. Nonetheless, in various real systems, the input vector is unknown and needs to be estimated simultaneously with the state vector. Also, in dynamic models with UBB uncertainties, the unknown center of the ellipsoidal set increases the state estimation complexity. “Unknown manoeuvre command estimation of a manoeuvring target tracking (MTT)”, “input disturbance estimation in motion control systems”, and the variable load on mechanical systems” are some of applications of unknown input and disturbance estimation problem. Unknown input and disturbance estimation is studied by researchers [16–18], in [19] the input estimation is used for estimation of the target maneuver input. In [20], designing and analysis of unknown input observer are presented in pursuance of estimation both unknown input and state vector in a complex dynamic system. In [21] and [22], the simultaneous unknown input and state vector estimation for discrete-time linear dynamic systems is proposed. Estimation of the unknown maneuver for the linear manoeuvring target tracking problem in the presence of UBB disturbances is studied in [23].

In spite of its various applications, the problem of “unknown input” and “disturbance” estimation in UBB uncertain systems is not studied considerably. Therefore, in this study, the problem of simultaneous estimation of the unknown input, disturbance, and state vector is studied for a special class of the nonlinear uncertain dynamical systems in the presence of the UBB uncertainties. In the design of the proposed estimator the concepts such as interval analysis, theory of closed convex sets, ellipsoidal over-approximation, and Holders inequality are used to achieve a proper mathematical form of proposed estimator. The designed estimator can be implemented on-line and its stability and boundedness is analysed. To achieve the above-mentioned goals, the remaining parts of this paper are structured as follows. In Sect. 2, the problem of unknown input and disturbance estimation is formulated. In Sect. 3, the main results are presented and the developed dynamic model and associated set value observer are presented and in Sect. 4, the stability of the proposed method is analyzed. Numerical simulations are done in Sect. 5 to verify the efficiency of the developed method and Sect. 6 presents the conclusions of this paper.

2 Unknown input and disturbance estimation problem

Consider a special class of uncertain nonlinear dynamical system with state space representation as follows:

$$\boldsymbol{x}_{k+1} = f(\boldsymbol{x}_k) + \boldsymbol{B}_k\boldsymbol{u}_k + \boldsymbol{G}_k\boldsymbol{w}_k \tag{1}$$

$$z_{k+1} = h(\boldsymbol{x}_{k+1}) + \boldsymbol{v}_{k+1} \tag{2}$$

where $\boldsymbol{x}_k \epsilon \mathbb{R}^{\boldsymbol{n}}$ is the dynamic system state vector, $\boldsymbol{u}_k \epsilon \mathbb{R}^{\boldsymbol{m}}$ is the input vector, $z_{k+1} \epsilon \mathbb{R}^{\boldsymbol{l}}$ is the observation vector, $\boldsymbol{w}_k \epsilon \mathbb{R}^{\boldsymbol{m}}$ is the exogenous process uncertainty or disturbance, and $\boldsymbol{v}_{k+1} \epsilon \mathbb{R}^{\boldsymbol{l}}$ is the exogenous observation disturbance. In this dynamic system, f and h are C^2 functions, $\boldsymbol{B}_k$ and $\boldsymbol{G}_k$ are $n \times m$ matrices. This system has three unknown but bounded uncertainties; initial state vector, process, and observation exogenous uncertainties. These uncertainties are modelled based on the UBB approach for uncertainty modelling. In this approach, each uncertainty is modelled with a convex closed set. In this study, ellipsoidal sets are used for uncertainty modelling as follows:

$$\boldsymbol{x}_0 \epsilon \boldsymbol{\Omega}_{x_0} = \{\boldsymbol{x} : \left(\boldsymbol{x} - \hat{\boldsymbol{x}}_0\right)^T \boldsymbol{\Sigma}_{0|0}^{-1}(\boldsymbol{x} - \hat{\boldsymbol{x}}_0) \leq 1 \tag{3}$$

$$\boldsymbol{w}_k \epsilon \boldsymbol{\Omega}_{w_k} = \left\{\boldsymbol{w} : (\boldsymbol{w} - \boldsymbol{w}_{c_k})^T \mathbf{Q}_k^{-1}(\boldsymbol{w} - \boldsymbol{w}_{c_k}) \leq 1\right\} \tag{4}$$

$$\boldsymbol{v}_k \epsilon \boldsymbol{\Omega}_{v_k} = \left\{\boldsymbol{v} : \left(\boldsymbol{v} - \boldsymbol{v}_{c_k}\right)^T \mathbf{R}_k^{-1}\left(\boldsymbol{v} - \boldsymbol{v}_{c_k}\right) \leq 1\right\} \tag{5}$$

where $\boldsymbol{\Sigma}_{0|0}$, $\boldsymbol{Q}_k$, and $\boldsymbol{R}_k$ are symmetric positive definite shaping matrices and $\hat{\boldsymbol{x}}_0$, $\boldsymbol{w}_{c_k}$, and $\boldsymbol{v}_{c_k}$ are the centres of the ellipsoidal sets $\boldsymbol{\Omega}_{x_0}$, $\boldsymbol{\Omega}_{w_k}$, and $\boldsymbol{\Omega}_{v_k}$ respectively. Any assumption is not considered about the structure of these uncertainties except that the values of the disturbances are bounded with the predefined ellipsoidal sets. The input and disturbance estimation problem consist of obtaining on-line estimation of $\hat{\boldsymbol{x}}_{k|k}$ based on observations from first sample time up to k sample time, subject to that disturbances $\boldsymbol{w}_{c_k}$ and input $\boldsymbol{u}_k$ are unknown. Therefore, in this problem the state vector, unknown input, and disturbance must be estimated simultaneously. It is considered that the shaping matrixes of process and observation disturbances are known and the centre of exogenous process disturbance is unknown. The solution of this problem when $\boldsymbol{w}_{c_k}$ and $\boldsymbol{u}_k$ are known is given by the extended set value observer (ESVO).

3 Main results

In this section, at first some materials that used in the evolution of the proposed method is presented and then the proposed method is illustrated.

3.1 Preliminaries

In the evolution of UBB-based observers such as ESVO, the below Lemmas are useful.

Lemma 1 *The affine or linear transformation of an ellipsoidal set with center* $\boldsymbol{q}$ *and shaping matrix* $\boldsymbol{Q}$ *is calculated as follows:*

$$\boldsymbol{A}\varepsilon(\boldsymbol{q}.\boldsymbol{Q})+\boldsymbol{b}\equiv\varepsilon\left(\boldsymbol{A}\boldsymbol{q}+\boldsymbol{b},\,\boldsymbol{A}\,\boldsymbol{Q}\,\boldsymbol{A}^{T}\right)\tag{6}$$

where $\boldsymbol{A}$ *and the* $\boldsymbol{b}$ *have appropriate dimensions.*

Proof See [24]. □

Lemma 2 *Consider ellipsoidal sets* $\boldsymbol{\Omega}_q$ *and* $\boldsymbol{\Omega}_r$ *as follows:*

$$\boldsymbol{\Omega}_q=\varepsilon(\boldsymbol{q},\boldsymbol{Q})=\{\boldsymbol{x}:(\boldsymbol{x}-\boldsymbol{q})^T\boldsymbol{Q}^{-1}(\boldsymbol{x}-\boldsymbol{q})\le 1\}$$
$$\boldsymbol{\Omega}_r=\varepsilon(\mathbf{r},\boldsymbol{R})=\{\boldsymbol{x}:(\boldsymbol{x}-\boldsymbol{r})^T\boldsymbol{R}^{-1}(\boldsymbol{x}-\boldsymbol{r})\le 1\}$$

The Minkowski sum of these sets are defined as follows:

$$\boldsymbol{\Omega}_{q+r}=\boldsymbol{\Omega}_q\oplus\boldsymbol{\Omega}_r=\{\boldsymbol{x}:\boldsymbol{x}\epsilon\boldsymbol{\Omega}_q\ or\ \boldsymbol{x}\epsilon\boldsymbol{\Omega}_r\}$$

where $\boldsymbol{\Omega}_{q+r}$ *is not ellipsoidal sets in general, but the determined set can be over approximated by ellipsoidal set as follows:*

$$\begin{aligned}\boldsymbol{\Omega}_{q+r}&=\boldsymbol{\Omega}_q\oplus\boldsymbol{\Omega}_r\subseteq\boldsymbol{\Omega}_b=\left\{\boldsymbol{x}:(\boldsymbol{x}-\boldsymbol{b})^T\boldsymbol{B}^{-1}(\boldsymbol{x}-\boldsymbol{b})\le 1\right\}\\ \boldsymbol{b}&=\boldsymbol{q}+\boldsymbol{r},\boldsymbol{B}=\frac{\boldsymbol{Q}}{\beta}+\frac{\boldsymbol{R}}{1-\beta},0\le\beta\le 1\end{aligned}\tag{7}$$

In (7), $\oplus$ is the Minkowski sum of two ellipsoids, and $\boldsymbol{\Omega}_b$ is the over-approximated ellipsoidal set that bonding the $\boldsymbol{\Omega}_{q+r}$

Proof Based on support function concept, Holder's inequality, and the convex combination of sets the relations (7) is proofed [5,25].

Lemma 3 *Consider* $\boldsymbol{\Omega}_q$ *and* $\boldsymbol{\Omega}_r$ *as ellipsoidal sets. The intersection of these sets is defined as follows:*

$$\boldsymbol{\Omega}_{q\cap r}=\boldsymbol{\Omega}_q\cap\boldsymbol{\Omega}_r=\{\boldsymbol{x}:\boldsymbol{x}\epsilon\boldsymbol{\Omega}_q\ and\ \boldsymbol{x}\epsilon\boldsymbol{\Omega}_r\}$$

where $\boldsymbol{\Omega}_{q\cap r}$ *is not ellipsoidal set in general, but the* $\boldsymbol{\Omega}_{q\cap r}$ *can be over approximated by ellipsoidal set as follows:*

$$\boldsymbol{\Omega}_q\cap\boldsymbol{\Omega}_r\subseteq\left\{\boldsymbol{x}\in\mathbb{R}^{\boldsymbol{n}}:[\boldsymbol{x}-\boldsymbol{b}]^T\boldsymbol{B}^{-1}[\boldsymbol{x}-\boldsymbol{b}]\le\left(1-\delta^2\right)\right\}\tag{8a}$$

$$\boldsymbol{B}=\left[(1-\rho)\,\boldsymbol{Q}^{-1}+\rho\mathbf{R}^{-1}\right]^{-1}\tag{8b}$$

$$\begin{aligned}\boldsymbol{b}&=\left(\frac{\boldsymbol{R}}{1-\rho}\left(\frac{\mathbf{Q}}{\rho}+\frac{\mathbf{R}}{1-\rho}\right)^{-1}\boldsymbol{q}\right.\\&\quad\left.+\frac{\mathbf{Q}}{\rho}\left(\frac{\mathbf{Q}}{\rho}+\frac{\mathbf{R}}{1-\rho}\right)^{-1}\boldsymbol{r}\right)\\&=\left(\boldsymbol{I}+\frac{1-\rho}{\rho}\mathbf{Q}\mathbf{R}^{-1}\right)^{-1}\boldsymbol{q}\\&\quad+\left(\boldsymbol{I}+\frac{\rho}{1-\rho}\mathbf{R}\mathbf{Q}^{-1}\right)^{-1}\boldsymbol{r}\end{aligned}\tag{8c}$$

$$\delta^2=\|\boldsymbol{q}-\boldsymbol{r}\|^2\left(\frac{\mathbf{Q}}{\rho}+\frac{\mathbf{R}}{1-\rho}\right)^{-1},0\le\rho\le 1\tag{8d}$$

Proof See [5,25].

3.2 Nonlinear dynamic model development

The uncertainties of the Eqs. (1) and (2) are defined by (3), (4), and (5). In this model, the center of the ellipsoidal sets is not zero. If these parameters (centre of ellipsoidal sets) are unknown, they can be considered as new state variables. By using Lemma 1, the system uncertainties can be rewritten as follows:

$$\begin{aligned}\boldsymbol{\Omega}_{w_k}&=\varepsilon\left(\boldsymbol{w}_{\boldsymbol{c}_k},\mathbf{Q}_k\right)=\boldsymbol{w}_{\boldsymbol{c}_k}+\varepsilon(0,\mathbf{Q}_k)\\ \bar{\bar{\boldsymbol{w}}}_{\boldsymbol{k}}\epsilon\bar{\bar{\Omega}}_{w_k}&=\varepsilon(0,\mathbf{Q}_k)=\left\{\bar{\bar{\boldsymbol{w}}}:\bar{\bar{\boldsymbol{w}}}_k^T\boldsymbol{Q}_k^{-1}\bar{\bar{\boldsymbol{w}}}_k\le 1\right\}\end{aligned}\tag{9}$$

$$\begin{aligned}\boldsymbol{\Omega}_{v_{k+1}}&=\varepsilon\left(\boldsymbol{v}_{\boldsymbol{c}_{k+1}},\mathbf{R}_{k+1}\right)=\boldsymbol{v}_{\boldsymbol{c}_{k+1}}+\varepsilon(0,\mathbf{R}_{k+1})\\ \bar{\bar{\boldsymbol{v}}}_{\boldsymbol{k+1}}\epsilon\bar{\bar{\Omega}}_{v_{k+1}}&=\varepsilon(0,\mathbf{R}_{k+1})\\&=\left\{\bar{\bar{\boldsymbol{v}}}:\bar{\bar{\boldsymbol{v}}}_{k+1}^T\boldsymbol{R}_{\boldsymbol{k+1}}^{-1}\bar{\bar{\boldsymbol{v}}}_{\boldsymbol{k+1}}\le 1\right\}\end{aligned}\tag{10}$$

Therefore the state equation is rearranged as follows:

$$\begin{aligned}\boldsymbol{x}_{k+1}&=f(\boldsymbol{x}_k)+\boldsymbol{B}_k\boldsymbol{u}_k+\boldsymbol{G}_k\boldsymbol{w}_k\\&=f(\boldsymbol{x}_k)+\boldsymbol{B}_k\boldsymbol{u}_k+\boldsymbol{G}_k\left(\boldsymbol{w}_{\boldsymbol{c}_k}+\bar{\bar{\boldsymbol{w}}}_k\right)\\&=f(\boldsymbol{x}_k)+\boldsymbol{B}_k\boldsymbol{u}_k+\boldsymbol{G}_k\boldsymbol{w}_{\boldsymbol{c}_k}\\&\qquad+\boldsymbol{G}_k\bar{\bar{\boldsymbol{w}}}_k\end{aligned}\tag{11}$$

$$z_{\boldsymbol{k+1}}=h(\boldsymbol{x}_{\boldsymbol{k+1}})+\boldsymbol{v}_k=h(\boldsymbol{x}_k)+\boldsymbol{v}_{\boldsymbol{c}_k}+\bar{\bar{\boldsymbol{v}}}_k\tag{12}$$

If $\boldsymbol{w}_{\boldsymbol{c}_k}$ and $\boldsymbol{u}_k$ are treated as augmented state variables, (11) can be converted to an augmented form as follows:

$$\tilde{\boldsymbol{x}}_{k+1} = \begin{bmatrix} \boldsymbol{x}_{k+1} \\ \boldsymbol{u}_{k+1} \\ \boldsymbol{w}_{\boldsymbol{c}_{k+1}} \end{bmatrix} + \begin{bmatrix} \boldsymbol{G}_k \\ \boldsymbol{0} \end{bmatrix} \bar{\bar{\boldsymbol{w}}}_k = \tilde{f}(\tilde{\boldsymbol{x}}_k) + \tilde{G}_k \bar{\bar{\boldsymbol{w}}}_k \tag{13}$$

where

$$\tilde{\boldsymbol{x}}_k = \begin{bmatrix} \boldsymbol{x}_k \\ \boldsymbol{u}_k \\ \boldsymbol{w}_{\boldsymbol{c}_k} \end{bmatrix}, \tilde{\boldsymbol{G}}_k = \begin{bmatrix} \boldsymbol{G}_k \\ \boldsymbol{0} \end{bmatrix},$$

$$\tilde{f}(\tilde{\boldsymbol{x}}_k) = \begin{bmatrix} f(\boldsymbol{x}_k) + \boldsymbol{B}_k \boldsymbol{u}_k + \boldsymbol{G}_k \boldsymbol{w}_{\boldsymbol{c}_k} \\ \boldsymbol{u}_k \\ \boldsymbol{w}_{\boldsymbol{c}_k} \end{bmatrix}$$

The Eq. (12) is rewritten as follows:

$$z_{k+1} = \tilde{h}(\tilde{\boldsymbol{x}}_{k+1}) + \bar{\bar{\boldsymbol{v}}}_{k+1}, \tilde{h}(\tilde{\boldsymbol{x}}_{k+1}) = h(\boldsymbol{x}_{k+1}) + \boldsymbol{v}_{\boldsymbol{c}_{k+1}} \tag{14}$$

Therefore, the augmented state space equations are described by (13) and (14).

3.3 The proposed set value observer

The structure of the proposed method for simultaneous estimation of unknown input, disturbance, and state vector is presented in this section. The proposed observer has prediction and time update steps. The estimated set for the system of Eqs. (13) and (14), is described as follows:

$$\begin{aligned}\boldsymbol{\Omega}_{\hat{\tilde{\boldsymbol{x}}}_{k+1|k+1}} &= \varepsilon\left(\hat{\tilde{\boldsymbol{x}}}_{k+1|k+1}, \boldsymbol{\Sigma}_{k+1|k+1}\right) \\ &= \left\{\tilde{\boldsymbol{x}} : [\tilde{\boldsymbol{x}} - \hat{\tilde{\boldsymbol{x}}}_{k+1|k+1}]^T \boldsymbol{\Sigma}^{-1}_{k+1|k+1}[\tilde{\boldsymbol{x}} \right. \\ &\qquad \left. - \hat{\tilde{\boldsymbol{x}}}_{k+1|k+1}] \le 1\right\}\end{aligned} \tag{15}$$

In (15), $\hat{\tilde{\boldsymbol{x}}}_{k+1|k+1}$ is the centre of the estimated set and $\boldsymbol{\Sigma}_{k+1|k+1}$ is the shaping matrix of this set. In the prediction step, the predicted set defined as follows:

$$\begin{aligned}\boldsymbol{\Omega}_{\hat{\tilde{\boldsymbol{x}}}_{k+1|k}} &= \varepsilon\left(\hat{\tilde{\boldsymbol{x}}}_{k+1|k}, \boldsymbol{\Sigma}_{k+1|k}\right) \\ &= \left\{\tilde{\boldsymbol{x}} : [\tilde{\boldsymbol{x}} - \hat{\tilde{\boldsymbol{x}}}_{k+1|k}]^T \boldsymbol{\Sigma}^{-1}_{k+1|k}[\tilde{\boldsymbol{x}} - \hat{\tilde{\boldsymbol{x}}}_{k+1|k}] \le 1\right\}\end{aligned} \tag{16}$$

3.3.1 Prediction step

• The interval of the augmented state vector is calculated based on the ellipsoidal extrema as follows:

$$\bar{X}^i_k = \left[\hat{\tilde{x}}^i_{k|k} - \sqrt{\boldsymbol{\Sigma}^{i.i}_{k|k}} \quad \hat{\tilde{x}}^i_{k|k} + \sqrt{\boldsymbol{\Sigma}^{i.i}_{k|k}}\right], i = 1 \ldots n \tag{17}$$

the index i denotes the ith component of the state vector.

• The maximum interval for the linearization remainder of the process equation is calculated. The process equation expanding, yields; e.g. for one state situation:

$$\begin{aligned}\tilde{f}(\tilde{\boldsymbol{x}}_k) &= \tilde{f}\left(\hat{\tilde{\boldsymbol{x}}}_{k|k}\right) + \left(\nabla_{\tilde{x}_k} \tilde{f}\left(\hat{\tilde{\boldsymbol{x}}}_{k|k}\right)\right)^T \left(\tilde{\boldsymbol{x}}_k - \hat{\tilde{\boldsymbol{x}}}_{k|k}\right) \\ &\quad + \frac{1}{2}\left(\tilde{\boldsymbol{x}}_k - \hat{\tilde{\boldsymbol{x}}}_{k|k}\right)^T \frac{\partial^2 \tilde{f}(\xi)}{\partial \tilde{x}^2_k}\left(\tilde{\boldsymbol{x}}_k - \hat{\tilde{\boldsymbol{x}}}_{k|k}\right)\end{aligned} \tag{18}$$

where $\nabla_{\tilde{x}_k} \tilde{f}(\tilde{\boldsymbol{x}}_k)$ is gradient of the $\tilde{f}$, $\frac{\partial^2 \tilde{f}}{\partial \tilde{x}^2_k}$ is second derivative of f, and $\boldsymbol{\xi}$ can take any value on the interval $\bar{X}_k$. Therefore, the interval of the remainder is calculated as follows:

$$\begin{aligned}&R_2\left(\tilde{x}_k - \hat{\tilde{x}}_{k|k} \cdot \bar{X}_k\right) \\ &= \frac{1}{2}\left(\tilde{\boldsymbol{x}}_k - \hat{\tilde{\boldsymbol{x}}}_{k|k}\right)^T \frac{\partial^2 \tilde{f}(\bar{X}_k)}{\partial \tilde{\boldsymbol{x}}^2_k}\left(\tilde{\boldsymbol{x}}_k - \hat{\tilde{\boldsymbol{x}}}_{k|k}\right)\end{aligned} \tag{19}$$

This relation for the n-states dynamic system is as follows:

$$\begin{aligned}X_{R_k} &= \frac{1}{2} diag\left(\left(\bar{X}_k - \hat{\tilde{x}}_k\right)^T\right)\begin{pmatrix} Hes\,\tilde{f}_1 \\ \vdots \\ Hes\,\tilde{f}_n \end{pmatrix}\left(\bar{X}_k - \hat{\tilde{x}}_k\right) \\ &= \frac{1}{2} diag\left(\Delta \bar{X}_k{}^T\right)\begin{pmatrix} Hes\,\tilde{f}_1 \\ \vdots \\ Hes\,\tilde{f}_n \end{pmatrix}\Delta \bar{X}_k{}^T\end{aligned} \tag{20}$$

where $Hes\,\tilde{f}_i$, $i = 1, 2 \ldots n$ is the Hessian of the nonlinear $\tilde{f}(.)$ and $\bar{X}_k$ is defined as $\bar{X}_k = \left(\bar{X}^1_k \cdot \bar{X}^2_k \ldots \bar{X}^n_k\right)$, and $\Delta \bar{X}_k$ is defined as $\Delta \bar{X}_k = \left(\sqrt{\boldsymbol{\Sigma}^{1.1}_{k|k}}, \sqrt{\boldsymbol{\Sigma}^{2.2}_{k|k}}, \ldots \sqrt{\boldsymbol{\Sigma}^{n.n}_{k|k}}\right)$

• Calculate the ellipsoid set that outer bounding the linearization error of process equation:

$$\varepsilon\left(\boldsymbol{0}_{n\times 1}, \bar{\boldsymbol{Q}}_k\right), [\bar{\boldsymbol{Q}}_k]^{i.i}_{R_k} = 2\left(X^i_{R_k}\right)^2, [\bar{\boldsymbol{Q}}_k]^{i.j}_{R_k} = \boldsymbol{0}_{n\times 1} \tag{21}$$

• Summation of the $\bar{\bar{\boldsymbol{\Omega}}}_w$ and $\varepsilon\left(\boldsymbol{0}_{n\times 1}.\bar{\boldsymbol{Q}}_k\right)$ is outer bounded by an ellipsoidal set based on Lemma. 2 as follows:

$$\begin{aligned}\hat{\boldsymbol{w}}_k \epsilon \boldsymbol{\Omega}_{\hat{w}} &= \varepsilon\left(\boldsymbol{0}_{n\times 1}, \hat{\boldsymbol{Q}}_k\right) = \left\{\hat{\boldsymbol{w}} : \hat{\boldsymbol{w}}^T \hat{\boldsymbol{Q}}_k^{-1} \hat{\boldsymbol{w}} \le 1\right\} \\ \hat{\boldsymbol{Q}}_k &= \boldsymbol{G}_k \frac{\boldsymbol{Q}_k}{\beta_{Q_k}} \boldsymbol{G}^T_k + \frac{\bar{\boldsymbol{Q}}_k}{1-\beta_{Q_k}}, 0 \le \beta_{Q_k} \le 1\end{aligned} \tag{22}$$

where

$$\begin{aligned}\boldsymbol{\Omega}_{\hat{\boldsymbol{w}}} &= \varepsilon\left(\boldsymbol{0}_{n\times 1}, \hat{\boldsymbol{Q}}_k\right) \supseteq \varepsilon\left(\boldsymbol{0}_{n\times 1}, \boldsymbol{G}_k \boldsymbol{Q}_k \boldsymbol{G}^T_k\right) \\ &\quad \oplus \varepsilon\left(\boldsymbol{0}_{n\times 1}, \bar{\boldsymbol{Q}}_k\right)\end{aligned} \tag{23}$$

Therefore, the linearized forme of the process equation is described as follows:

$$\tilde{\boldsymbol{x}}_{k+1} = \tilde{f}\left(\tilde{\boldsymbol{x}}_k\right) + \tilde{\boldsymbol{G}}_k \bar{\bar{\boldsymbol{w}}}_k \cong \boldsymbol{A}_k \tilde{\boldsymbol{x}}_k + \hat{\boldsymbol{w}}_k \tag{24}$$

• The prediction ellipsoidal set calculated as follows:

$$\varepsilon\left(\hat{\tilde{\boldsymbol{x}}}_{k+1|k}, \boldsymbol{\Sigma}_{k+1|k}\right) \supseteq \varepsilon\left(\tilde{f}\left(\hat{\tilde{\boldsymbol{x}}}_{k|k}\right), \boldsymbol{\Sigma}_{k|k}\right) \oplus \varepsilon\left(\boldsymbol{0}_{n\times 1}, \hat{\mathbf{Q}}_k\right) \tag{25}$$

$$\hat{\tilde{\boldsymbol{x}}}_{k+1|k} = \tilde{f}(\hat{\tilde{\boldsymbol{x}}}_{k|k}) \tag{26}$$

$$\boldsymbol{\Sigma}_{k+1|k} = \boldsymbol{A}_k \frac{\boldsymbol{\Sigma}_{k|k}}{1-\beta_k} \boldsymbol{A}_k^T + \frac{\hat{\mathbf{Q}}_k}{\beta_k}, 0 \le \beta_k \le 1 \tag{27}$$

$$\boldsymbol{A}_k = \left(\nabla_{\hat{x}_k} \tilde{f}\left(\tilde{\boldsymbol{x}}_k\right)\right)^T |_{\tilde{\boldsymbol{x}}_k = \hat{\tilde{\boldsymbol{x}}}_{k|k}} \tag{28}$$

3.3.2 Time update step

• Calculate the interval for the linearization remainder of the observation equation. Similar to the process remainder, the observation reminder is described as follows:

$$Z_{R_k} = \frac{1}{2} diag\left(\left(\bar{X}_k - \hat{\tilde{x}}_k\right)^T\right) \begin{pmatrix} Hes\tilde{h}_1 \\ \vdots \\ Hes\tilde{h}_n \end{pmatrix} \left(\bar{X}_k - \hat{\tilde{x}}_k\right) \tag{29}$$

• Calculate the ellipsoid set that outer bounding the linearization error of the observation equation:

$$\varepsilon\left(\boldsymbol{0}_{m\times 1}, \bar{\boldsymbol{R}}_k\right), \left[\bar{\boldsymbol{R}}_k\right]_{R_k}^{i.i} = 2\left(Z_{R_k}^i\right)^2, \left[\bar{\boldsymbol{R}}_k\right]_{R_k}^{i.j} = \boldsymbol{0}_{m\times 1} \tag{30}$$

• Bound summation of the observation noise ellipsoid set and $\varepsilon\left(\boldsymbol{0}_{m\times 1}, \bar{\boldsymbol{R}}_k\right)$:

$$\hat{\boldsymbol{v}}_k \epsilon \boldsymbol{\Omega}_{\hat{v}} = \varepsilon\left(\boldsymbol{0}_{m\times 1}, \hat{\mathbf{R}}_k\right) = \left\{\hat{\boldsymbol{v}} : \hat{\boldsymbol{v}}^T \hat{\mathbf{R}}_k^{-1} \hat{\boldsymbol{v}} \le 1\right\}$$

$$\hat{\mathbf{R}}_k = \frac{\mathbf{R}_k}{\beta_{R_k}} + \frac{\bar{\mathbf{R}}_k}{1-\beta_{R_k}}, 0 \le \beta_{R_k} \le 1 \tag{31}$$

where

$$\boldsymbol{\Omega}_{\hat{v}} = \varepsilon\left(\boldsymbol{0}_{m\times 1}, \hat{\mathbf{R}}_k\right) \supseteq \varepsilon\left(\boldsymbol{0}_{m\times 1}, \mathbf{R}_k\right) \oplus \varepsilon\left(\boldsymbol{0}_{m\times 1}, \bar{\mathbf{R}}_k\right) \tag{32}$$

Therefore the linearized form of the observation equation is described as follows:

$$z_{k+1} = \tilde{h}\left(\tilde{\mathbf{x}}_{k+1}\right) + \boldsymbol{v}_{\boldsymbol{c}_k} + \bar{\bar{\boldsymbol{v}}}_{k+1} \tag{33a}$$

If $\boldsymbol{v}_{\boldsymbol{c}_k} = 0$, then:

$$\begin{aligned} z_{k+1} &= \tilde{h}\left(\tilde{\boldsymbol{x}}_{k+1}\right) + \bar{\bar{\boldsymbol{v}}}_{k+1} = \boldsymbol{H}_{k+1}\tilde{\boldsymbol{x}}_{k+1} + \hat{\boldsymbol{v}}_{k+1} \\ &= \boldsymbol{H}_{k+1}\left(\boldsymbol{A}_k\tilde{\boldsymbol{x}}_k + \hat{\boldsymbol{w}}_k\right) + \hat{\boldsymbol{v}}_{k+1} \\ &= \boldsymbol{H}_{k+1}\boldsymbol{A}_k\tilde{\boldsymbol{x}}_k + \boldsymbol{H}_{k+1}\hat{\boldsymbol{w}}_k \\ &\quad + \hat{\boldsymbol{v}}_{k+1} + \boldsymbol{v}_{\boldsymbol{c}_k} = \tilde{\boldsymbol{H}}_{k+1}\tilde{\boldsymbol{x}}_k + \hat{\tilde{\boldsymbol{v}}}_{k+1} \end{aligned} \tag{33b}$$

where

$$\tilde{\boldsymbol{H}}_{k+1} = \boldsymbol{H}_{k+1}\boldsymbol{A}_k \tag{34}$$

$$\hat{\tilde{\boldsymbol{v}}}_{k+1} = \boldsymbol{H}_{k+1}\hat{\boldsymbol{w}}_k + \hat{\boldsymbol{v}}_{k+1} = \varepsilon\left(\boldsymbol{0}_{m\times 1}, \hat{\tilde{\mathbf{R}}}_k\right)$$

$$\hat{\tilde{\mathbf{R}}}_k = \frac{\boldsymbol{H}_{k+1}\boldsymbol{A}_k\hat{\boldsymbol{Q}}_k\boldsymbol{A}_k^T\boldsymbol{H}_{k+1}^{\boldsymbol{T}}}{\beta_{\tilde{R}_k}} + \frac{\hat{\mathbf{R}}_k}{1-\beta_{\tilde{R}_k}}, \quad 0 \le \beta_{\tilde{R}_k} \le 1 \tag{35}$$

• Calculate the observation update ellipsoidal set. It is derived by the intersection of the $\varepsilon\left(\hat{\tilde{\boldsymbol{x}}}_{k+1|k}, \boldsymbol{\Sigma}_{k+1|k}\right)$ and the observation ellipsoidal set as follows:

$$\begin{aligned} \boldsymbol{\Omega}_{z|\tilde{x}_{k+1}} &= \varepsilon\left(\tilde{h}\left(\hat{\tilde{\boldsymbol{x}}}_{k+1|k}\right), \hat{\mathbf{R}}_k\right) \\ &= \left\{z : \left(z_{k+1} - \tilde{h}(\hat{\tilde{\boldsymbol{x}}}_{k+1|k})\right)^T \hat{\mathbf{R}}_k^{-1}\left(z_{k+1} \right.\right. \\ &\quad \left.\left. - \tilde{h}(\hat{\tilde{\boldsymbol{x}}}_{k+1|k})\right)^T \le 1\right\} \end{aligned} \tag{36}$$

Therefore, the estimated set described as follows:

$$\varepsilon\left(\hat{\tilde{\boldsymbol{x}}}_{k+1|k+1}, \boldsymbol{\Sigma}_{k+1|k+1}\right) \supseteq \varepsilon\left(\hat{\boldsymbol{x}}_{k+1|k}, \boldsymbol{\Sigma}_{k+1|k}\right) \cap \varepsilon\left(\tilde{h}\left(\hat{\tilde{\boldsymbol{x}}}_{k+1|k}\right), \hat{\mathbf{R}}_k\right) \tag{37}$$

Moreover, with some calculus manipulations, the equations of the observation update step described as follows:

$$\hat{\tilde{\boldsymbol{x}}}_{k+1|k+1} = \tilde{f}\left(\hat{\tilde{\boldsymbol{x}}}_{k|k}\right) + \boldsymbol{K}_{k+1}\left[z_{k+1} - \tilde{\boldsymbol{h}}(\hat{\tilde{\boldsymbol{x}}}_{k+1|k})\right] \tag{38}$$

$$\boldsymbol{\Sigma}_{k+1|k+1} = \left[1 - \delta_{k+1}^2\right]\boldsymbol{\Sigma}_{b_{k+1|k+1}} \tag{39}$$

$$\boldsymbol{K}_{k+1} = \boldsymbol{\Sigma}_{b_{k+1|k+1}}\tilde{\boldsymbol{H}}_{k+1}^T\tilde{\boldsymbol{R}}_{k+1}^{-1} \tag{40}$$

$$\boldsymbol{\Sigma}_{b_{k+1|k+1}} = \tilde{\boldsymbol{\Sigma}}_{k+1|k} - \tilde{\boldsymbol{\Sigma}}_{k+1|k}\tilde{\boldsymbol{H}}_{k+1}^T\left\{\tilde{\boldsymbol{R}}_{k+1} + \tilde{\boldsymbol{H}}_{k+1}\tilde{\boldsymbol{\Sigma}}_{k+1|k}\tilde{\boldsymbol{H}}_{k+1}^T\right\}^{-1}\tilde{\boldsymbol{H}}_{k+1}\tilde{\boldsymbol{\Sigma}}_{k+1|k} \tag{41}$$

$$\tilde{\boldsymbol{\Sigma}}_{k+1|k} = \left[\frac{1}{1-\rho_{k+1}}\right]\boldsymbol{\Sigma}_{k+1|k}, 0 \le \rho_{k+1} \le 1 \tag{42}$$

$$\tilde{\boldsymbol{R}}_k = \frac{1}{\rho_k}\hat{\tilde{\boldsymbol{R}}}_k, \; \tilde{\boldsymbol{Q}}_k = \frac{1}{\beta_k}\hat{\boldsymbol{Q}}_k \tag{43}$$

$$\delta_{k+1}^2 = \left[z_{k+1} - \tilde{h}\left(\hat{\tilde{\boldsymbol{x}}}_{k+1|k}\right)\right]^T \left\{\tilde{\boldsymbol{H}}_{k+1}\tilde{\boldsymbol{\Sigma}}_{k+1|k}\tilde{\boldsymbol{H}}_{k+1}^T + \tilde{\boldsymbol{R}}_{k+1}\right\}^{-1} \left[z_{k+1} - \tilde{h}\left(\hat{\tilde{\boldsymbol{x}}}_{k+1|k}\right)\right] \tag{44}$$

$$\hat{\tilde{\boldsymbol{x}}}_{0|0} = \boldsymbol{0} \tag{45}$$

$$\boldsymbol{H}_{k+1} = \left(\nabla_{x_{k+1}}\tilde{h}\left(\tilde{x}_{k+1}\right)\right)^T |_{\tilde{x}_{k+1}} = \hat{\tilde{\boldsymbol{x}}}_{k+1|k} \tag{46}$$

These equations give a recursive form for the estimation of the unknown input, disturbance, and state vector.

Remark 1 This observer has five free parameters; i.e. β_{Q_k}, β_k, β_{R_k}, $\beta_{\tilde{R}_k}$ and ρ_{k+1}. The improper selection of these free parameters can dramatically degrade the estimation performance. Therefor the proper selection of these free parameters must be considered in the observer implementation.

Remark 2 By using interval analysis, the linearization reminder is considered in the development of the linearized forme of dynamic system equations. The linearized model is described as illustrated in (47) and (48):

$$\tilde{\boldsymbol{x}}_{k+1} = \boldsymbol{A}_k\tilde{\boldsymbol{x}}_k + \hat{\boldsymbol{w}}_k \tag{47}$$

$$z_{k+1} = \tilde{\boldsymbol{H}}_{k+1}\tilde{\boldsymbol{x}}_k + \hat{\tilde{\boldsymbol{v}}}_{k+1} \tag{48}$$

The uncertainties $\hat{\boldsymbol{w}}_k$ and $\hat{\tilde{\boldsymbol{v}}}_{k+1}$, models the combination of exogenous process and observation disturbances and linearization reminder. For achieving proper linearized form of observation equation, it is rearranged and the above form is obtained and the $\tilde{\boldsymbol{x}}_k$ is appeared in (48) instead of $\tilde{\boldsymbol{x}}_{k+1}$.

Remark 3 In (39) and (44), the shaping matrix $(\boldsymbol{\Sigma}_{k+1|k+1})$ of the estimated set $(\boldsymbol{\Omega}_{\hat{\tilde{x}}_{k+1|k+1}})$ is dependent on the observations. Therefore, in the analysis of this observer, this shaping matrix cannot be used. Due to this problem, usually $\boldsymbol{\Sigma}_{b_{k+1|k+1}}$ is used for analysis of the proposed observer estimation performance.

3.4 Calculation of the estimator free parameters

In the development of the proposed method, five free parameters (β_{Q_k}, β_k, β_{R_k}, $\beta_{\tilde{R}_k}$ and ρ_{k+1}) are appeared. All of these free parameters must be lie in the interval (0, 1). In this section, a method for suboptimal selection of these parameters is presented [26]. These parameters appear when an ellipsoidal set is over approximated to the intersection or Minkowski sum of two ellipsoidal sets. Assume that two ellipsoids are defined as $\varepsilon(\boldsymbol{a}_1, \boldsymbol{P}_1)$ and $\varepsilon(\boldsymbol{a}_2, \boldsymbol{P}_2)$, while the covered ellipsoid of their direct sum is $\varepsilon(\boldsymbol{a}, \boldsymbol{P})$. By using Lemma 2, **a** and **P** can be selected as

$$a = \theta\boldsymbol{a}_1 + (1-\theta)\,\boldsymbol{a}_2,\ \boldsymbol{P} = \frac{\boldsymbol{P}_1}{1-\theta} + \frac{\boldsymbol{P}_2}{\theta},\quad 0 \le \theta \le 1 \tag{49}$$

To select the optimal value for θ the goal of the optimization is defined as follows:

$$\theta = \underset{\theta\in(0,1)}{\arg}\ \min Tr(\boldsymbol{P}) \tag{50}$$

The optimal value of θ can be selected as [27]:

$$\theta = \frac{\sqrt{Tr(\boldsymbol{P}_2)}}{\sqrt{Tr(\boldsymbol{P}_1)} + \sqrt{Tr(\boldsymbol{P}_2)}} \tag{51}$$

Therefore the β_{Q_k}, β_k, β_{R_k}, $\beta_{\tilde{R}_k}$ calculated based on (51).

To determine the optimal value of the ρ_{k+1}, the matrix $\tilde{\boldsymbol{\Sigma}}_{k+1|k+1} = \left[1-\delta^2_{k+1}\right]\boldsymbol{\Sigma}_{b_{k+1|k+1}}$ is considered. Where δ^2_{k+1} described in (44). By maximizing the δ^2_{k+1}, the trace of $\tilde{\boldsymbol{\Sigma}}_{k+1|k+1}$ is minimized. Based on this criteria, in [27] the optimal value of ρ_{k+1} is derived:

$$\rho_{k+1} = \frac{\sqrt{r_m}}{\sqrt{p_m} + \sqrt{r_m}} \tag{52}$$

where p_m, and r_m are maximum singular values of the matrix $\tilde{\boldsymbol{H}}_{k+1}\tilde{\Sigma}_{k+1|k}\tilde{\boldsymbol{H}}^T_{k+1}$ and $\tilde{\boldsymbol{R}}_{k+1}$.

4 Stability analysis

As been mentioned, feasible sets are the output of the designed estimator. The centre of the estimated sets is considered as estimation vectors. Therefore, in the stability analysis of the proposed method, two problems must be considered; "converges of the estimation error" and the "boundedness of the estimated set".

4.1 Estimation error ISS stability

Consider the linearized form of the dynamic system as shown in (47) and (48). Where $\hat{\boldsymbol{w}}_k$ and $\hat{\tilde{\boldsymbol{v}}}_{k+1}$ are defined in (22) and (35). The estimation error is defined in (53):

$$\boldsymbol{\zeta}_{k+1} = \tilde{\boldsymbol{x}}_{k+1} - \hat{\tilde{\boldsymbol{x}}}_{k+1|k+1}, \tag{53a}$$

$$\boldsymbol{\zeta}_{k+1|k} = \tilde{\boldsymbol{x}}_{k+1} - \hat{\tilde{\boldsymbol{x}}}_{k+1|k} \tag{53b}$$

Then

$$\begin{aligned}\boldsymbol{\zeta}_{k+1} &= \tilde{\boldsymbol{x}}_{k+1} - \hat{\tilde{\boldsymbol{x}}}_{k+1|k+1}\\ &= \boldsymbol{A}_k\tilde{\boldsymbol{x}}_k + \hat{\boldsymbol{w}}_k - \Big[\boldsymbol{A}_k\hat{\tilde{\boldsymbol{x}}}_{k|k}\\ &\quad - \Big(z_{k+1} - \tilde{\boldsymbol{H}}_{k+1}\boldsymbol{A}_k\hat{\tilde{\boldsymbol{x}}}_{k|k}\Big)\Big]\\ &= \Big(\boldsymbol{A}_k - \boldsymbol{K}_{k+1}\tilde{\boldsymbol{H}}_{k+1}\Big)\boldsymbol{\zeta}_k + \hat{w}_k\\ &\quad -\boldsymbol{K}_{k+1}\hat{\tilde{\boldsymbol{v}}}_{k+1} = \tilde{\boldsymbol{A}}_k\boldsymbol{\zeta}_k + \boldsymbol{r}_{k+1}\end{aligned} \tag{54}$$

where

$$\boldsymbol{r}_{k+1} = \hat{w}_k - \boldsymbol{K}_{k+1}\hat{\tilde{\boldsymbol{v}}}_{k+1} \tag{55}$$

$$\tilde{\boldsymbol{A}}_k = \Big(\boldsymbol{A}_k - \boldsymbol{K}_{k+1}\tilde{\boldsymbol{H}}_{k+1}\Big) \tag{56}$$

And the predicted estimation error is determined as follows

$$\begin{aligned}\boldsymbol{\zeta}_{k+1|k} &= \tilde{\boldsymbol{x}}_{k+1} - \hat{\tilde{\boldsymbol{x}}}_{k+1|k} = \boldsymbol{A}_k\tilde{\boldsymbol{x}}_k + \hat{\boldsymbol{w}}_k\\ &\quad -\boldsymbol{A}_k\hat{\tilde{\boldsymbol{x}}}_{k|k} = \boldsymbol{A}_k\boldsymbol{\zeta}_k + \hat{\boldsymbol{w}}_k\end{aligned} \tag{57}$$

Equations (54) and (57) show the estimation error propagation respect to time. These dynamic systems are linear perturbed systems. The stability of the perturbed systems is established by ISS-Lyapunov stability. In (54), $\boldsymbol{r}_{k+1}$ is as UUB uncertainty that calculated as follows

$$\boldsymbol{r}_{k+1} \in \varepsilon\left(0, \boldsymbol{P}_{k+1}\right) = \varepsilon\left(0, \frac{\hat{\mathbf{Q}}_k}{1-\lambda_{k+1}} + \frac{\boldsymbol{K}_{k+1}\hat{\mathbf{R}}_{k+1}\boldsymbol{K}_{k+1}^T}{\lambda_{k+1}}\right) \tag{58}$$

where $0 \leq \lambda_{k+1} \leq 1$.

Definition 1 The $\boldsymbol{x}_{k+1} = f(\boldsymbol{x}_k.\boldsymbol{u}_k)$ is ISS if $\nu(\boldsymbol{x}) : R^n \to R_+$ is a Lyapunov function such that for all $\boldsymbol{x} \epsilon R^n$ and $\boldsymbol{u} \epsilon R^m$ [28]:

$$\begin{aligned} &\nu(\boldsymbol{x}) \text{ continuously differentiable} \\ &\quad \alpha_1(\|\boldsymbol{x}\|) \leq \nu(\boldsymbol{x}) \leq \alpha_2(\|\boldsymbol{x}\|), \alpha_1 \textit{ and } \alpha_2 \\ &\quad \textit{are } k_\infty \text{ functions} \end{aligned} \tag{59}$$

$$\begin{aligned} &\nu(f(\boldsymbol{x}_k, \boldsymbol{u}_k)) - \nu(\boldsymbol{x}_k) \leq -\alpha_3(\|\boldsymbol{x}_k\|) + \alpha_u(\|\boldsymbol{u}_k\|), \alpha_3 \\ &\quad \text{is } k_\infty \text{ and } \alpha_u \text{ is } k \text{ functions} \end{aligned} \tag{60}$$

Lemma 4 *If the pair* $(\boldsymbol{A}_k, \tilde{\boldsymbol{H}}_{k+1})$ *be uniformly observable, the real numbers* $\underline{s}$, $\underline{\acute{s}}$, $\bar{s}$, *and* $\bar{\acute{s}}$ *are exist such that*

$$\underline{s} \times \boldsymbol{I} \leq \boldsymbol{\Sigma}_{k|k-1} \leq \bar{s} \times \boldsymbol{I}, \underline{\acute{s}} \times \boldsymbol{I} \leq \boldsymbol{\Sigma}_{k|k} \leq \bar{\acute{s}} \times \boldsymbol{I} \tag{61}$$

Proof See [29]

Theorem 1 *Suppose that the following assumptions hold:*

1. *The pair* $(\boldsymbol{A}_k, \tilde{\boldsymbol{H}}_{k+1})$ *is uniformly observable.*
2. *The* $\boldsymbol{A}_k$, *and* $\tilde{\boldsymbol{H}}_{k+1}$ *are invertible for all* $k \geq 0$.
3. $\|\boldsymbol{A}_k\| \leq \bar{a}$, *and* $\left\|\tilde{\mathbf{H}}_{k+1}\right\| \leq \bar{h}$

Then the estimator error dynamics (50) and (53) are ISS.

Proof For ISS stability, conditions (55) and (56) must be satisfied. The Lyapunov functions are defined as follows:

$$\nu_{\boldsymbol{k}}\left(\zeta_{k+1|k}\right) = \boldsymbol{\zeta}_{k+1|k}^T \boldsymbol{\Sigma}_{k+1|k}^{-1} \boldsymbol{\zeta}_{k+1|k} \tag{62}$$

$$\nu_{\boldsymbol{k}}\left(\zeta_{k+1}\right) = \boldsymbol{\zeta}_{k+1}^T \boldsymbol{\Sigma}_{k+1|k+1}^{-1} \boldsymbol{\zeta}_{k+1} \tag{63}$$

From (57), it is obvious that:

$$\underline{s} \times \boldsymbol{I} \leq \boldsymbol{\Sigma}_{k+1|k} \leq \bar{s} \times \boldsymbol{I} => \frac{\left\|\boldsymbol{\zeta}_{k+1|k}\right\|^2}{\underline{s}} \geq \boldsymbol{\zeta}_{k+1|k}^T \boldsymbol{\Sigma}_{k+1|k}^{-1} \boldsymbol{\zeta}_{k+1|k} \geq \frac{\left\|\boldsymbol{\zeta}_{k+1|k}\right\|^2}{\bar{s}} \tag{64}$$

Therefore, by defining

$$\alpha_1(\|\boldsymbol{x}\|) = \frac{\left\|\boldsymbol{\zeta}_{k+1|k}\right\|^2}{\bar{s}}, \alpha_2(\|\boldsymbol{x}\|) = \frac{\left\|\boldsymbol{\zeta}_{k+1|k}\right\|^2}{\underline{s}} \tag{65}$$

the condition (55) is satisfied as follows:

$$\alpha_1(\|\boldsymbol{x}\|) \leq \nu_{\boldsymbol{k}}\left(\boldsymbol{\zeta}_{k+1|k}\right) \leq \alpha_2(\|\boldsymbol{x}\|)$$

The proof of the

$$\alpha_1(\|\boldsymbol{x}\|) \leq \nu_{\boldsymbol{k}}\left(\boldsymbol{\zeta}_{k+1}\right) \leq \alpha_2(\|\boldsymbol{x}\|)$$

is achieved in a similar way. To verify the second condition for ISS-stability, the Lyapunov function is calculated.

$$\begin{aligned} \nu\left(\boldsymbol{\zeta}_{k+1|k}\right) &= \left(\boldsymbol{A}_k\boldsymbol{\zeta}_k + \hat{\boldsymbol{w}}_k\right)^T \boldsymbol{\Sigma}_{k+1|k}^{-\mathbf{1}} \left(\boldsymbol{A}_k\boldsymbol{\zeta}_k + \hat{\boldsymbol{w}}_k\right) \\ &= \left(\boldsymbol{\zeta}_k^T\boldsymbol{A}_k^T + \hat{\boldsymbol{w}}_k^T\right)\left[\boldsymbol{A}_k\frac{\boldsymbol{\Sigma}_{k|k}}{1-\beta_k}\boldsymbol{A}_k^T + \frac{\hat{\mathbf{Q}}_k}{\beta_k}\right]^{-\mathbf{1}} \\ &\quad \left(\boldsymbol{A}_k\boldsymbol{\zeta}_k + \hat{\boldsymbol{w}}_k\right) \\ &\leq \left(\boldsymbol{\zeta}_k^T\boldsymbol{A}_k^T + \hat{\boldsymbol{w}}_k^T\right)\left[\left(1-\beta_k\right)\boldsymbol{A}_k^{-T}\boldsymbol{\Sigma}_{k|k}^{-1}\boldsymbol{A}_k^{-1} \right. \\ &\quad \left. + \beta_k\hat{\mathbf{Q}}_k^{-1}\right]\left(\boldsymbol{A}_k\boldsymbol{\zeta}_{k+1} + \hat{\boldsymbol{w}}_k\right) \\ &\leq \left(1-\beta_k\right)\left(\boldsymbol{A}_k\boldsymbol{\zeta}_{k+1}\right)^T \boldsymbol{A}_k^{-T}\boldsymbol{\Sigma}_{k|k}^{-1}\boldsymbol{A}_k^{-1}\left(\boldsymbol{A}_k\boldsymbol{\zeta}_{k+1}\right) \\ &\quad + \beta_k\hat{\boldsymbol{w}}_k^T\hat{\mathbf{Q}}_k^{-1}\hat{\boldsymbol{w}}_k \leq \left(1-\beta_k\right)\boldsymbol{\zeta}_k^T\boldsymbol{\Sigma}_{k|k}^{-1}\boldsymbol{\zeta}_k \\ &\quad + \beta_k\hat{\boldsymbol{w}}_k^T\hat{\mathbf{Q}}_k^{-1}\hat{\boldsymbol{w}}_k \\ &\leq \left(1-\beta_k\right)\nu\left(\boldsymbol{\zeta}_{k|k}\right) + \beta_k\hat{\boldsymbol{w}}_k^T\hat{\mathbf{Q}}_k^{-1}\hat{\boldsymbol{w}}_k \end{aligned} \tag{66}$$

It is obvious that [15]:

$$\nu\left(\boldsymbol{\zeta}_{k+1|k+1}\right) - \nu\left(\boldsymbol{\zeta}_{k|k}\right) \leq \nu\left(\boldsymbol{\zeta}_{k+1|k}\right) - \nu\left(\boldsymbol{\zeta}_{k|k}\right) \tag{67}$$

By adding ν, the below relation is derived:

$$\begin{aligned} \nu\left(\boldsymbol{\zeta}_{k+1|k+1}\right) - \nu\left(\boldsymbol{\zeta}_{k|k}\right) &\leq \nu\left(\boldsymbol{\zeta}_{k+1|k}\right) - \nu\left(\boldsymbol{\zeta}_{k|k}\right) \\ &\leq \left(1-\beta_k\right)\nu\left(\boldsymbol{\zeta}_{k|k}\right) + \beta_k\hat{\boldsymbol{w}}_k^T\hat{\boldsymbol{Q}}_k^{-1}\hat{\boldsymbol{w}}_k \\ &\quad - \nu\left(\boldsymbol{\zeta}_{k|k}\right) \\ &= -\beta_k\nu\left(\boldsymbol{\zeta}_{k|k}\right) + \beta_k\hat{\boldsymbol{w}}_k^T\hat{\boldsymbol{Q}}_k^{-1}\hat{\boldsymbol{w}}_k \\ &\leq \frac{-\beta_k\left\|\boldsymbol{\zeta}_{k|k}\right\|^2}{eig_{min}\left(\boldsymbol{\Sigma}_{k|k}\right)} + \frac{\beta_k\left\|\hat{\boldsymbol{w}}_k\right\|^2}{eig_{min}\left(\hat{\boldsymbol{w}}_k\right)} \end{aligned} \tag{68}$$

Therefore, the below relation is satisfied

$$\nu\left(\boldsymbol{\zeta}_{k+1|k+1}\right) - \nu\left(\boldsymbol{\zeta}_{k|k}\right) \leq \frac{-\beta_k\left\|\boldsymbol{\zeta}_{k|k}\right\|^2}{eig_{min}\left(\boldsymbol{\Sigma}_{k|k}\right)} + \frac{\beta_k\left\|\hat{\boldsymbol{w}}_k\right\|^2}{eig_{min}\left(\hat{\boldsymbol{w}}_k\right)} \tag{69}$$

by defining

$$\alpha_3(\|\boldsymbol{x}_k\|) = \frac{\beta_k\left\|\boldsymbol{\zeta}_{k|k}\right\|^2}{eig_{min}\left(\boldsymbol{\Sigma}_{k|k}\right)}, \alpha_u(\|\boldsymbol{u}_k\|) = \frac{\beta_k\left\|\hat{\boldsymbol{w}}_k\right\|^2}{eig_{min}\left(\hat{\boldsymbol{w}}_k\right)}$$

The (69) is satisfied the second condition of the Lyapunov ISS-stability.

4.2 Boundedness A of the estimation error

It is guaranteed that the actual state vector is a member of the estimated set that defined in (15). Therefore, it is needed that the boundedness of the sets is analyzed.

Lemma 5 *Suppose that*

1. $\boldsymbol{M}, \boldsymbol{C}, \boldsymbol{D}$, *and* $\boldsymbol{E}$ *are general matrices.*
2. $\boldsymbol{C}\boldsymbol{C}^T \leq I$ *and* $\boldsymbol{X}$ *is a PSD matrix.*
3. α *is a positive constant*
4. $\alpha^{-1}\boldsymbol{I} - \boldsymbol{E}\boldsymbol{X}\boldsymbol{E}^T > 0$.

Therefore the below relation holds:

$$(\boldsymbol{M} + \boldsymbol{C}\boldsymbol{D}\boldsymbol{E})\,\boldsymbol{X}\,(\boldsymbol{M} + \boldsymbol{C}\boldsymbol{D}\boldsymbol{E})^T \leq \boldsymbol{M}\left(\boldsymbol{X}^{-1} - \alpha \boldsymbol{E}\boldsymbol{E}^T\right)^{-1}\boldsymbol{M}^T + \alpha^{-1}\boldsymbol{C}\boldsymbol{C}^T \tag{70}$$

Proof of Lemma 4 see [30]

By replacing $\boldsymbol{M}$ with $\boldsymbol{A}_k$, $\boldsymbol{C}$ with $\boldsymbol{I}$, $\boldsymbol{D}$ with $\boldsymbol{0}$, $\boldsymbol{E}$ with $\boldsymbol{I}$, and $\boldsymbol{X}$ with $\boldsymbol{\zeta}_k\boldsymbol{\zeta}_k^T$, (70) is rearranged as follows:

$$\boldsymbol{A}_k\boldsymbol{\zeta}_k\boldsymbol{\zeta}_k^T\boldsymbol{A}_k^T \leq \boldsymbol{A}_k\left(\left(\boldsymbol{\zeta}_k\boldsymbol{\zeta}_k^T\right)^{-1} - \alpha_1\boldsymbol{I}\right)^{-1}\boldsymbol{A}_k^T + \alpha_1^{-1}\boldsymbol{I} \tag{71}$$

By using the inverse lemma

$$\boldsymbol{A}_k\boldsymbol{\zeta}_k\boldsymbol{\zeta}_k^T\boldsymbol{A}_k^T \leq \boldsymbol{A}_k[\boldsymbol{\zeta}_k\boldsymbol{\zeta}_k^T + \boldsymbol{\zeta}_k\boldsymbol{\zeta}_k^T(\boldsymbol{\alpha}_1^{-1}\boldsymbol{I} - \boldsymbol{\zeta}_k\boldsymbol{\zeta}_k^T)^{-1}\boldsymbol{\zeta}_k\boldsymbol{\zeta}_k^T]\boldsymbol{A}_k^T + \alpha_1^{-1}\boldsymbol{I} \tag{72}$$

The relation (70) can be rewritten as follows:

$$\frac{\boldsymbol{A}_k\boldsymbol{\zeta}_k\boldsymbol{\zeta}_k^T\boldsymbol{A}_k^T}{1-\beta_k} + \frac{\hat{\boldsymbol{Q}}_k}{\beta_k} \leq (1-\beta_k)^{-1}\left[\boldsymbol{A}_k\left[\boldsymbol{\zeta}_k\boldsymbol{\zeta}_k^T + \boldsymbol{\zeta}_k\boldsymbol{\zeta}_k^T\left(\alpha_1^{-1}\boldsymbol{I} - \boldsymbol{\zeta}_k\boldsymbol{\zeta}_k^T\right)^{-1}\boldsymbol{\zeta}_k\boldsymbol{\zeta}_k^T\right]\boldsymbol{A}_k^T - \alpha_1^{-1}\boldsymbol{I}\right] + \beta_k^{-1}\hat{\boldsymbol{Q}}_k \tag{73}$$

By definition

$$\mathbf{P}_{k+1|k} = \frac{\boldsymbol{A}_k\boldsymbol{\zeta}_k\boldsymbol{\zeta}_k^T\boldsymbol{A}_k^T}{1-\beta_k} + \frac{\hat{\boldsymbol{Q}}_k}{\beta_k} \tag{74}$$

Now the upper bound for $\mathbf{P}_{k+1|k}$ described as follows:

$$\mathbf{P}_{k+1|k} \leq (1-\beta_k)^{-1}\left[\boldsymbol{A}_k\left[\boldsymbol{\zeta}_k\boldsymbol{\zeta}_k^T + \boldsymbol{\zeta}_k\boldsymbol{\zeta}_k^T\left(\alpha_1^{-1}\boldsymbol{I} - \boldsymbol{\zeta}_k\boldsymbol{\zeta}_k^T\right)^{-1}\boldsymbol{\zeta}_k\boldsymbol{\zeta}_k^T\right]\boldsymbol{A}_k^T - \alpha_1^{-1}\boldsymbol{I}\right] + \beta_k^{-1}\hat{\boldsymbol{Q}}_k \tag{75}$$

The relation between brackets can be reformulated:

$$[\boldsymbol{\zeta}_k\boldsymbol{\zeta}_k^T + \boldsymbol{\zeta}_k\boldsymbol{\zeta}_k^T(\alpha_1^{-1} - \boldsymbol{\zeta}_k\boldsymbol{\zeta}_k^T)^{-1}\boldsymbol{\zeta}_k\boldsymbol{\zeta}_k^T \leq \boldsymbol{\zeta}_k(1-\alpha_1)\boldsymbol{\zeta}_k^T = (1-\alpha_1)\boldsymbol{\zeta}_k\boldsymbol{\zeta}_k^T \tag{76}$$

Therefore, the upper bound of the $\mathbf{P}_{k+1|k}$ is as follows:

In a similar way, the upper bound for $\mathbf{P}_{k+1|k+1}$ is calculated:

$$\mathbf{P}_{k+1|k} \leq \frac{\boldsymbol{A}_k\boldsymbol{\zeta}_k\boldsymbol{\zeta}_k^T\boldsymbol{A}_k^T + \alpha_1^{-1}\boldsymbol{I}}{(1-\alpha_1)^{-1}(1-\beta_k)} + \frac{\hat{\boldsymbol{Q}}_k}{\beta_k} = \frac{\boldsymbol{A}_k\mathbf{P}_{k|k}\boldsymbol{A}_k^T + \alpha_1^{-1}\boldsymbol{I}}{(1-\alpha_1)^{-1}(1-\beta_k)} + \frac{\hat{\boldsymbol{Q}}_k}{\beta_k} \tag{77}$$

$$\mathbf{P}_{k+1|k+1} = \boldsymbol{\zeta}_{k+1}\boldsymbol{\zeta}_{k+1}^T \tag{78}$$

$$\mathbf{P}_{k+1|k+1} \leq \frac{\left(\boldsymbol{I} - \boldsymbol{K}_{k+1}\tilde{\boldsymbol{H}}_{k+1}\right)\mathbf{P}_{k+1|k}\left(\boldsymbol{I} - \boldsymbol{K}_{k+1}\tilde{\boldsymbol{H}}_{k+1}\right)^T}{(\boldsymbol{1}-\boldsymbol{\alpha}_1)^{-1}(\boldsymbol{1}-\boldsymbol{\beta}_k)} + \boldsymbol{K}_{k+1}\left(\frac{\hat{\tilde{\boldsymbol{R}}}_{k+1}}{\boldsymbol{\rho}_k}\right)\boldsymbol{K}_{k+1}^T \tag{79}$$

It is obvious that

$$\mathbf{P}_{k+1|k} \leq \boldsymbol{\Sigma}_{k+1|k} = \boldsymbol{A}_k\frac{\boldsymbol{\Sigma}_{k|k}}{1-\beta_k}\boldsymbol{A}_k^T + \frac{\hat{\mathbf{Q}}_k}{\beta_k} \tag{80}$$

$$\mathbf{P}_{k+1|k+1} \leq \boldsymbol{\Sigma}_{b_{k+1|k+1}} = \tilde{\boldsymbol{\Sigma}}_{k+1|k} - \tilde{\boldsymbol{\Sigma}}_{k+1|k}\tilde{\boldsymbol{H}}_{k+1}^T\{\tilde{\boldsymbol{R}}_{k+1} + \tilde{\boldsymbol{H}}_{k+1}\tilde{\boldsymbol{\Sigma}}_{k+1|k}\tilde{\boldsymbol{H}}_{k+1}^T\}^{-1}\tilde{\boldsymbol{H}}_{k+1}\tilde{\boldsymbol{\Sigma}}_{k+1|k} \tag{81}$$

5 Numerical simulations

In this section, to demonstrate the efficiency of the developed method, the performance of the unknown input and disturbance estimation are examined for two different nonlinear dynamical systems.

Example 1 In this example a nonlinear dynamic system with below state space equations is studied:

$$\boldsymbol{x}_{k+1} = f(\boldsymbol{x}_k) + \boldsymbol{B}_k u_k + \boldsymbol{G}_k w_k \tag{82}$$

$$y_{k+1} = \boldsymbol{H}_{k+1}\boldsymbol{x}_{k+1} + v_{k+1} \tag{83}$$

$$\boldsymbol{x}_{k+1} = [x_k \quad \dot{x}_k]^T = \left[x_{1_k} \quad x_{2_k}\right]^T \tag{84}$$

$$f(\boldsymbol{x}_{k+1}) = \begin{bmatrix} x_{1_k} + T x_{2_k} \\ x_{2_k} + T\left(-\frac{k_0}{m}x_{1_k}\left(1 + k_d x_{1_k}^2\right) - \frac{c}{m}x_{2_k}\right) \end{bmatrix} \tag{85}$$

Table 1 Numerical simulation constants and parameters

Parameter	Value	Parameter	Value
T	0.01 (s)	Q	0.01
m	1 (kg)	R	0.01
k_0	1.5	k_d	3
c	1.2	$\boldsymbol{\Sigma}_{0\|0}$	$0.01I_{2\times2}$

$$\boldsymbol{H}_{k+1}=\begin{bmatrix}0.1 & 0\end{bmatrix},\quad \boldsymbol{B}_k=\begin{bmatrix}0\\ \frac{1}{m}\end{bmatrix},\quad \boldsymbol{G}_k=\begin{bmatrix}1\\1\end{bmatrix} \tag{86}$$

where T is the sample time, x_k or x_{1_k} is the position in m, $\dot{x}_k$ or x_{2_k} is the velocity in m/s, k_0, k_d, and c are constant parameters. The observation is y_{k+1}, and u_k is the unknown input. In this system, w_k and $v_{k+1}$are the input and observation disturbances respectively. In this model the input and disturbance are considered as unknown variables.

$$w_k\epsilon\Omega_w=\left\{w:\left(w-w_{c_k}\right)^T \mathrm{Q}_k^{-1}\left(w-w_{c_k}\right)\le 1\right\} \tag{87}$$

$$v_k\epsilon\Omega_v=\{v:(v-v_{c_k})^T\mathrm{R}_k^{-1}(v-v_{c_k})\le 1\} \tag{88}$$

The system parameters are as those that illustrated in Table 1. In this example the free parameters are as follows:

$$\beta_{Q_k}=0.5,\quad \beta_k=0.5,\quad \beta_{R_k}=0.001,\quad \beta_{\tilde{R}_k}=0.01,$$
$$\rho_{k+1}=0.01$$

First, the input is considered unknown and the disturbance is neglected. Therefore the u_k is changed as a step-like input from zero to 0.1. The $[0(\mathrm{m}),0(\mathrm{m/s})]^T$ is the initial state vector, and $w_{ck}=v_{c_k}=0$. For comparing proposed methods with other input estimation methods, the simulation results are compared with unknown input observer (UIO) method that was proposed in [31,32].

For the parameters that illustrated in the Table 1, the simulations are down and results are presented in Figs. 1, 2 and 3. In Figs. 1 and 2, the real and estimated values for dynamic system state vector are illustrated. In Fig. 1a, the actual values of x_{1_k} and its estimated values are presented. In Fig. 1b, the estimation error of the x_{1_k} are presented. In Fig. 2a, the actual and the estimated values of x_{2_k} are presented. In Fig. 2b, the estimation error of x_{2_k} is depicted. In Fig. 3a, the actual and estimated values of unknown input and in Fig. 3b, the estimation errors of the unknown input for proposed method are illustrated. These figures are showing acceptable performance of the proposed method in estimation of the state vector and unknown input. In comparison to the UIO method, the proposed method shows better performance in estimation of the state vector and unknown input.

In the second scenario of this example, the unknown input and disturbance are estimated simultaneously with state vector. The simulation parameters are similar those that are illustrated in Table 1. In this simulation, the unknown input and disturbance are changed sinusoidal and ramp like respectively as illustrated in Figs. 4 and 5. In Fig. 4a, the actual unknown input and its estimated values for proposed and UIO methods are shown. In Fig. 4b, unknown input estimation error is presented for the above-mentioned methods. In Fig. 5a, the disturbance and its estimated values are shown. In Fig. 5b, the disturbance estimation error is illustrated. These figures are showing the acceptable performance of the proposed method in the unknown input and disturbance estimation. The proposed method estimation error of unknown input and disturbance are negligible. As it is obvious, the proposed method estimation precisely tracks the actual value of the unknown input and disturbance. Moreover, the proposed method performance in the state vector estimation is significantly better than UIO method.

Finally, in the third part of Example 1, another simulation is done to find out the effect of the filter free parameters on the state estimation of the proposed method. In this simulation, only the parameters β_{Q_k} and ρ_{k+1} are changed as illustrated in Fig. 6. The simulation results are depicted on Fig. 6. As it is obvious, the change in the filter parameters directly affect on the estimation accuracy. In Fig. 6b, the estimation error for various parameters are shown.

Example 2 In this example, the input estimation for the nonlinear MTT problem is studied. The dynamic model of the manoeuvring target tracking problem is as follows:

$$\begin{cases}\boldsymbol{x}_{k+1}=\boldsymbol{F}_k\boldsymbol{x}_k+\boldsymbol{B}_k\boldsymbol{u}_k+\boldsymbol{G}_k\boldsymbol{w}_k\\ \boldsymbol{z}_{k+1}=\boldsymbol{h}\left(\boldsymbol{x}_{k+1}\right)+\boldsymbol{v}_{k+1}\end{cases} \tag{89}$$

where, $\boldsymbol{x}_{k+1}$ is the target state vector, $\boldsymbol{u}_k$ is the unknown target manoeuvre, $\boldsymbol{w}_k$ and $\boldsymbol{v}_{k+1}$ are the process and observation noises respectively. The x and v_x are target position and velocity in the x-axis and so others. The state vector defined as follows:

$$\boldsymbol{x}_k=\begin{bmatrix}\boldsymbol{x}_k & \boldsymbol{v}_{x_k} & \boldsymbol{y}_k & \boldsymbol{v}_{y_k} & \boldsymbol{z}_k & \boldsymbol{v}_{z_k}\end{bmatrix}^T \tag{90}$$

$$\boldsymbol{u}_k=[\boldsymbol{u}_{x_k}\ \ \boldsymbol{u}_{y_k}\ \ \boldsymbol{u}_{z_k}]^T \tag{91}$$

$$\boldsymbol{F}_k=\begin{bmatrix}1 & T & 0 & 0 & 0 & 0\\ 0 & 1 & 0 & 0 & 0 & 0\\ 0 & 0 & 1 & T & 0 & 0\\ 0 & 0 & 0 & 1 & 0 & 0\\ 0 & 0 & 0 & 0 & 1 & T\\ 0 & 0 & 0 & 0 & 0 & 1\end{bmatrix},\quad \boldsymbol{B}_k=\begin{bmatrix}\frac{T^2}{2} & 0 & 0\\ T & 0 & 0\\ 0 & \frac{T^2}{2} & 0\\ 0 & T & 0\\ 0 & 0 & \frac{T^2}{2}\\ 0 & 0 & T\end{bmatrix},$$

$$\boldsymbol{G}_k=\begin{bmatrix}1\\1\\1\\1\\1\\1\end{bmatrix} \tag{92}$$

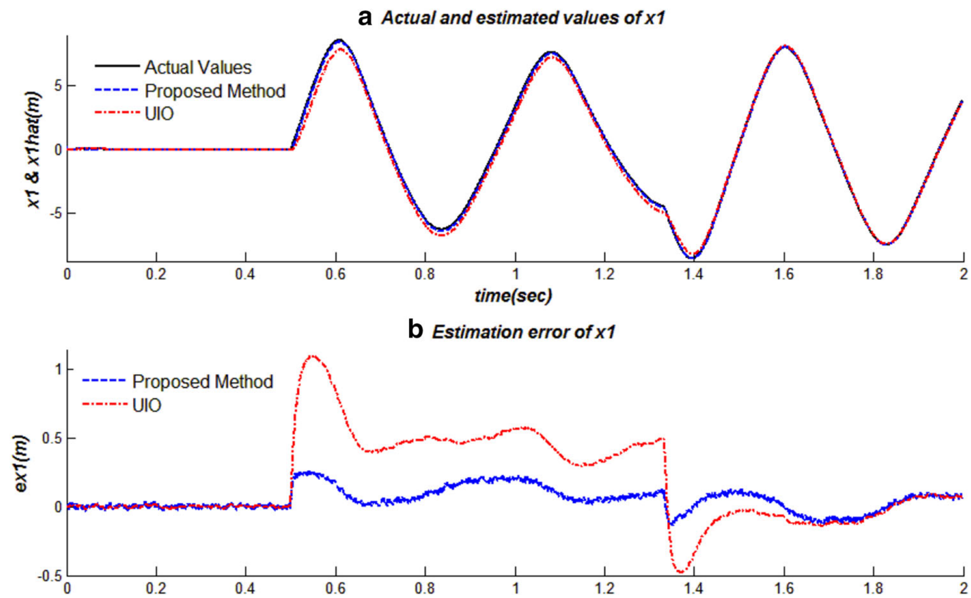

Fig. 1 Simulation results of Example 1 in the estimation of state vector; **a** estimated and actual values of x_{1_k}; **b** x_{1_k} estimation error

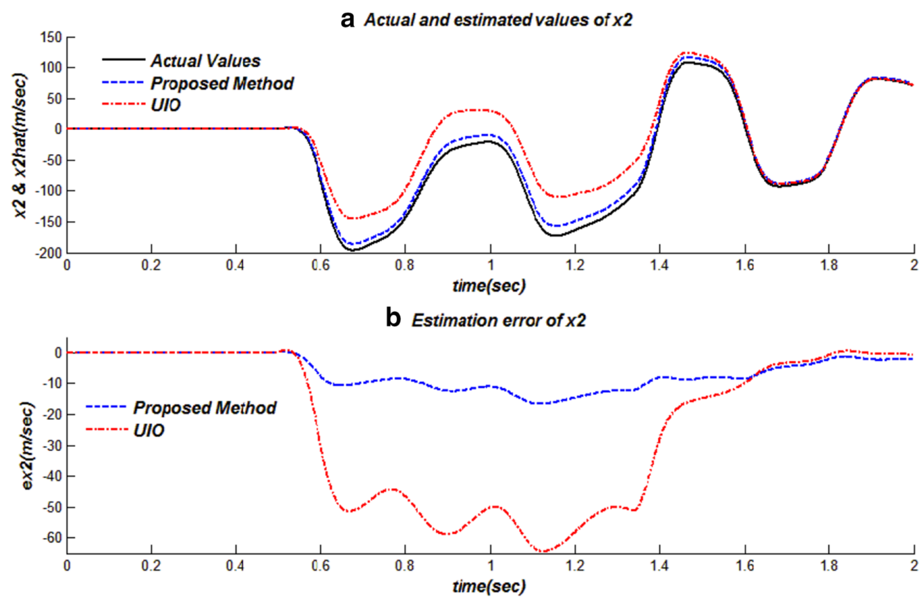

Fig. 2 Simulation results of Example 1 in the estimation of state vector; **a** estimated and actual values of x_{2_k}; **b** x_{2_k} estimation error

Tracking sensor measurers the target bearing angle (φ_k), elevation angle (θ_k), and range (r_k). The nonlinear function $h(\boldsymbol{x}_k)$ is defined as follows:

$$z_{k+1} = \begin{bmatrix} \varphi_{k+1} \\ \theta_{k+1} \\ r_{k+1} \end{bmatrix} = \boldsymbol{h}(\boldsymbol{x}_{k+1}) = \begin{cases} atan\left(\frac{y_{k+1}}{x_{k+1}}\right) \\ atan\left(\frac{z_{k+1}}{r_{k+1}}\right) \\ \sqrt{x_{k+1}^2 + y_{k+1}^2 + z_{k+1}^2} \end{cases} \tag{93}$$

In this simulation, the estimation of the target maneuver is considered. It is supposed that, the target is an Aircraft with [2000(m); 50(m/s); 2000(m); −50(m/s)] as initial state vector, $T = 0.001$ s, $\boldsymbol{R}$, $\boldsymbol{Q}$, and $\boldsymbol{\psi}$ are diagonal with $\boldsymbol{R}_{ii} = 10$, $\boldsymbol{Q}_{ii} = 0.1$, and $\boldsymbol{\psi}_{ii} = 1$ as diagonal elements. The target maneuver for time lower than 10*s* is zero and for other times it is $[-60; -60](\mathrm{m/s^2})$. In this example the filter free parameters are as follows:

$$\beta_{Q_k} = 0.05, \quad \beta_k = 0.07, \quad \beta_{R_k} = 0.995,$$
$$\beta_{\tilde{R}_k} = 0.001, \quad \rho_{k+1} = 0.01$$

In Fig. 7, the target maneuver estimation and its estimation error are presented for various noises. The actual and estimated values of target in x and y directions are shown in Fig. 7a, c respectively. The target maneuver estimation error is presented in Fig. 7b, d for x and y axis respectively. It is obvious that the proposed method estimates the target maneuver properly in x and y directions for various noises. The steady state error of estimated target maneuver is negli-

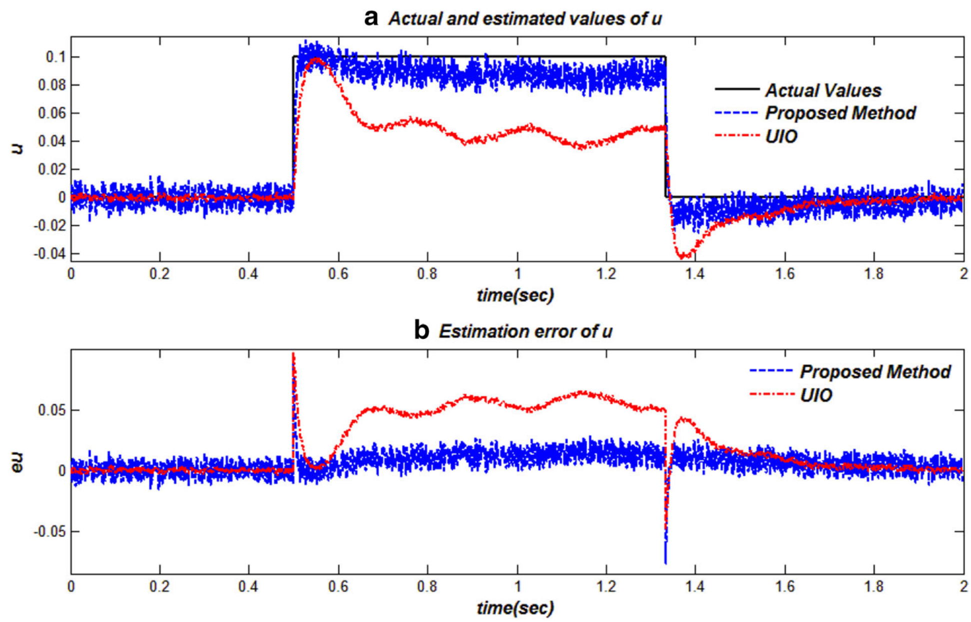

Fig. 3 Simulation results of Example 1 in the estimation of unknown input; **a** estimated and actual values of u_k; **b** u_k estimation error

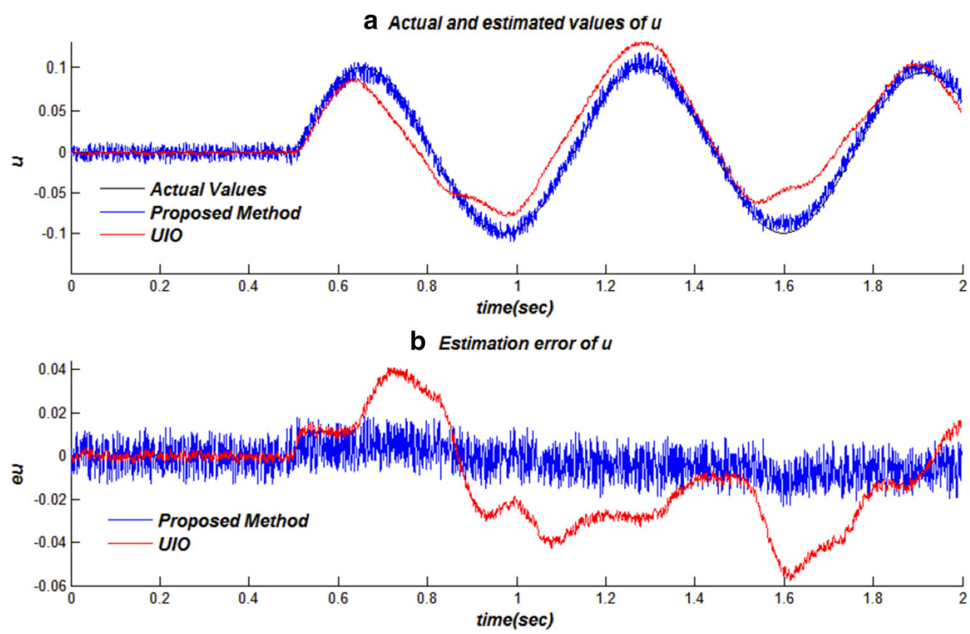

Fig. 4 Simulation results of Example 1 in the estimation of unknown input; **a** estimated and actual values of u_k; **b** u_k estimation error

gible for target tracking applications. The proposed method is robust in the presence of various noises.

In Fig. 8, the estimation of the target maneuver in the x-axis, for different target maneuvers is compared with input estimation (IE) and modified input estimation (MIE) methods [22,33]. In this figure four maneuver types (Step, Ramp, Sinusoidal, and hyperbolic) are presented. In this simulation, parameters are $T = 0.04s$, $\boldsymbol{R}_{ii} = 2$, $\boldsymbol{Q}_{ii} = 0.1$, *and* $\boldsymbol{\psi}_{ii} = 1$. In Fig. 8a, for a step-like maneuver, the actual values and estimated values for proposed method, IE method and MIE method are illustrated. In Fig. 8b–e drawings are presented for ramp, hyperbola, and sinusoidal maneuvers respectively. In all the target maneuver types, the proposed method has better accuracy and response time rather than other methods. In highly maneuvers, the MIE and IE methods failed on target maneuver tracking. Also, the maneuver estimation delay time of the proposed method is lower than IE and MIE methods especially in high maneuver scenarios. This simulation shows the effectiveness of the proposed method in another nonlinear dynamical system unknown input estimation.

Example 3 To quantitative verification of the proposed method, a Monte-Carlo simulation is performed for second part of Example 1. The simulations are performed for 200 runs, and in each run, the root-mean-square error is calculated. Subse-

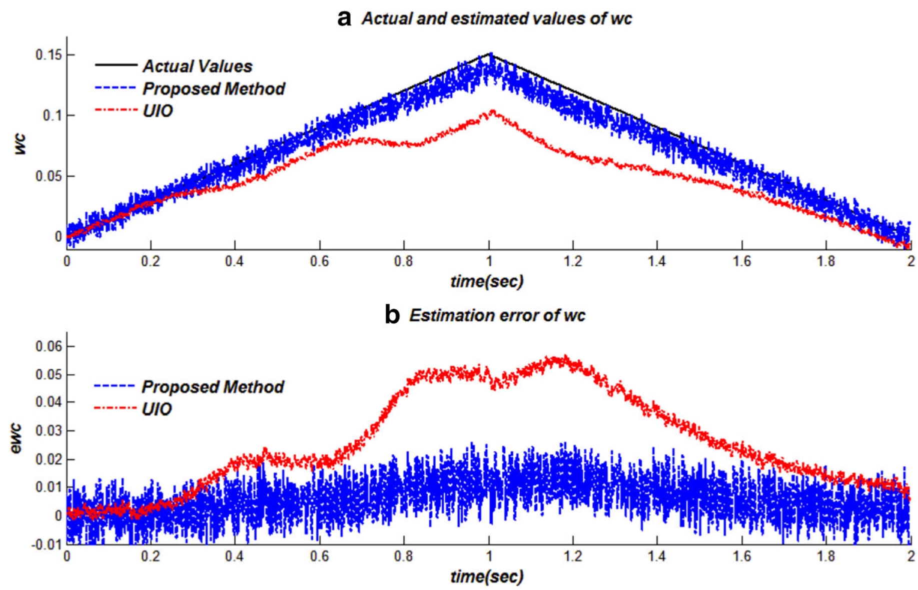

Fig. 5 Simulation results of Example 1 in the estimation of disturbance; **a** estimated and actual values of w_c; **b** w_c estimation error

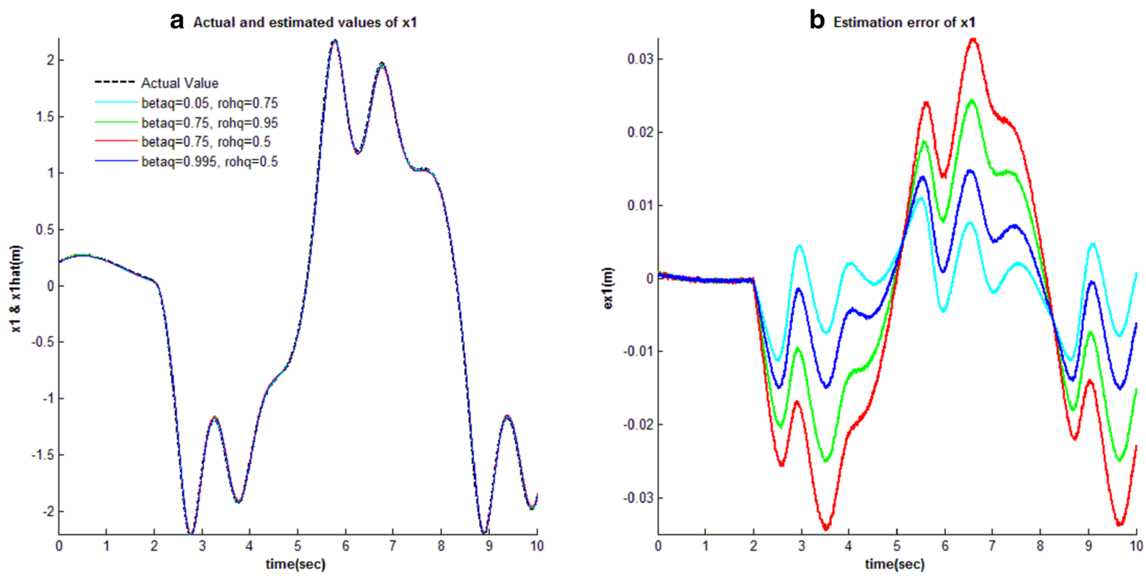

Fig. 6 Effect of free parameters on estimation of the x_{1k}; **a** estimation and actual values of x_{1k}; **b** x_{1k} estimation error

quently, the average estimation error for states and unknown input is calculated and presented in Table 2. The quantitative simulation results show that the proposed method exhibits better performance rather than UIO methods for the estimation of dynamic system position, velocity, and unknown input. To study the computation burden of the proposed method rather than other methods, in this simulation, the mean elapsed time for each iteration is calculated by using tic-toc command in Matlab software. As it is obvious, the computation burden of the proposed method is about 2 times greater than UIO method.

6 Conclusion

In this study, under the assumption of the UBB-based uncertainties and disturbances, an ellipsoidal-based extended set value observer is proposed for simultaneous estimation of the state vector, unknown input, and disturbance for a special class of nonlinear dynamical systems. If in a nonlinear system, the input or disturbances are unknown, the performance of the state vector estimation is degraded dramatically. In the proposed method, the unknown input and disturbance are considered augmented states and therefore a new state space model for the dynamical system is developed. By using the interval analysis, the linearization reminder of the pro-

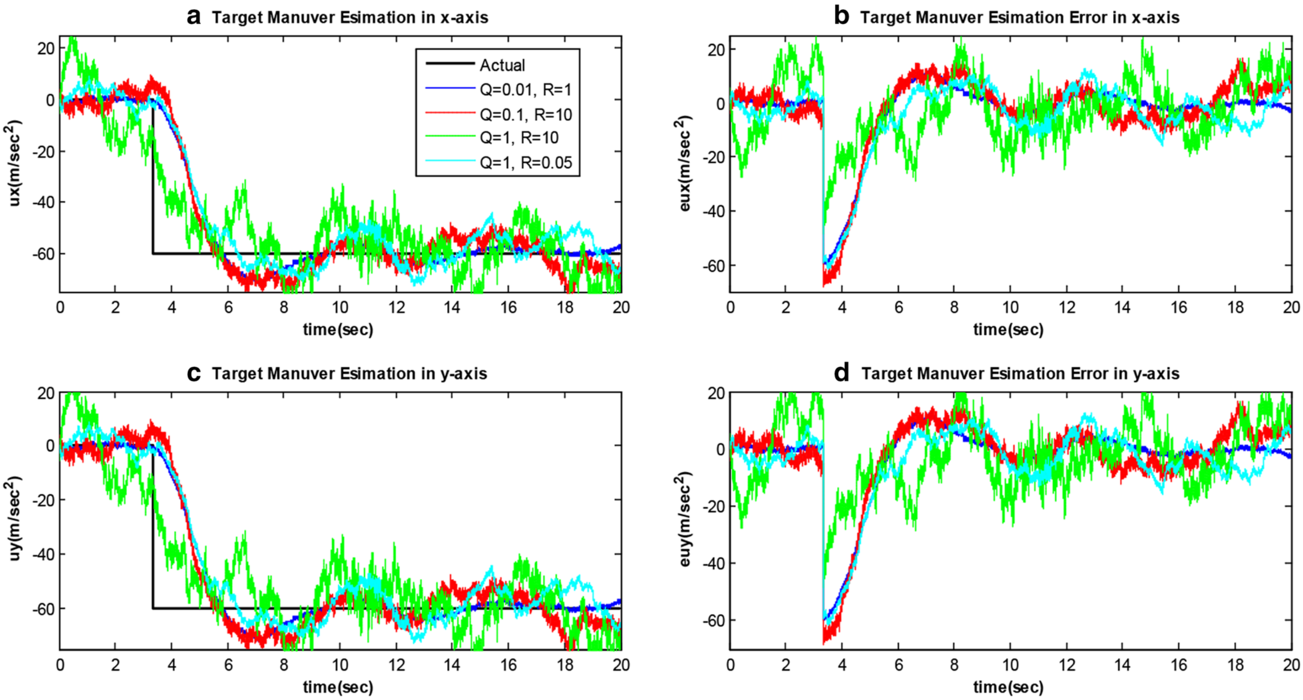

Fig. 7 Target manoeuvre estimation in x-axis and y-axis for Example 2

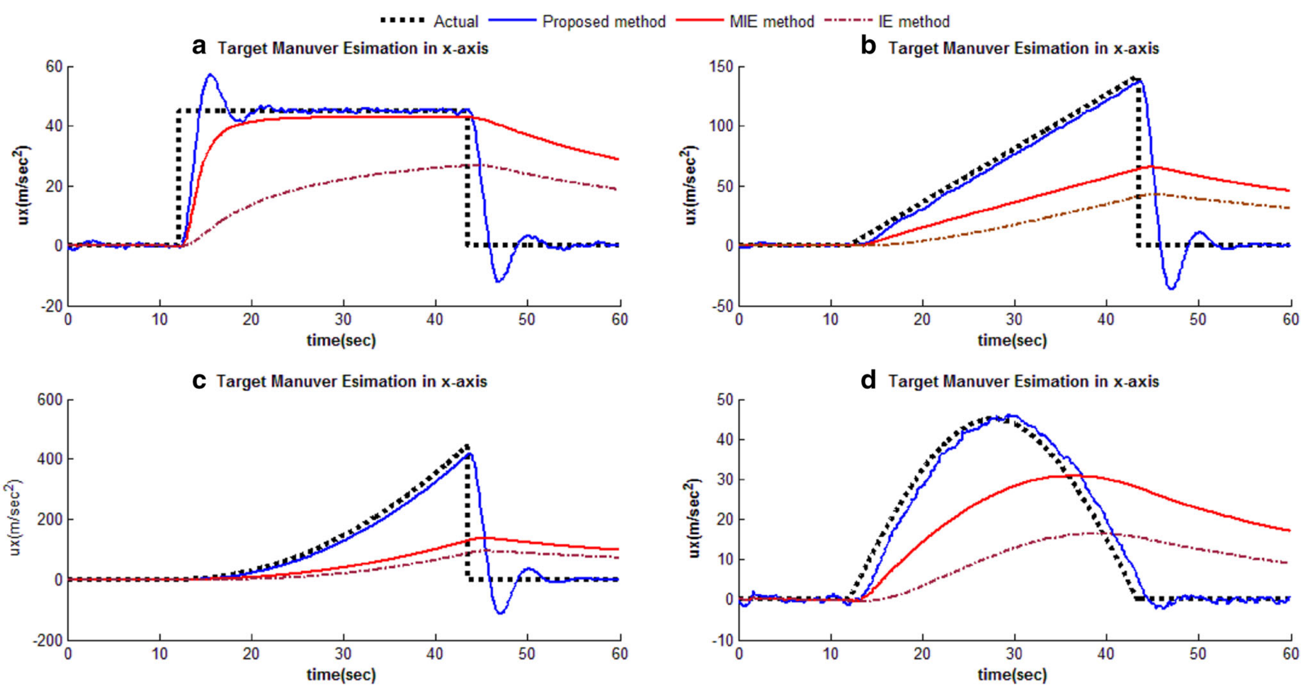

Fig. 8 Target manoeuvre estimation in x direction for Example 2 in various target manoeuvres

Table 2 Monte-Carlo simulation results for 200 runs

State	RMS error	
	UIO	Proposed method
x_1 : position (m)	2.45	4.55
x_2 : position (m)	758.83	175.19
u : force (N)	0.85	0.45
Mean computation time (ms)	0.1	0.22

cess and observation equations are considered in linearization process. These reminders are bounded by convex closed ellipsoidal sets, these ellipsoidal sets are combined with the system and observation uncertainties to achieving a proper form of the state space equations. To add augmented states in the observation equation, this equation is rearranged and a modified form of observation equation is developed. Based on the developed model and by using set value observer concept, the state, unknown input, and disturbance vectors are estimated simultaneously.

Furthermore, the stability of the proposed method is established. In the stability analysis, the convergence and boundedness of the estimation error are studied. The estimation error dynamics model is determined. The achieved error dynamic equation is a perturbed dynamic system, where the estimation error is its state vector and a linear combination of process and observation uncertainties is its perturbed input. Therefore, its ISS-Lyapunov stability must be satisfied. To analysis the ISS stability of the error dynamic, a proper Lyapunov function is selected and its stability is analyzed. Moreover, the boundedness of the estimation error is analyzed and an upper bound for estimation error is calculated. Therefore, the stability of the proposed estimator is completely satisfied.

To demonstrate the efficiency of the proposed algorithm, various numerical simulations are down. The simulations shown that the developed method can accurately estimate the state vector, unknown input, and disturbance simultaneously. In the simulations, the performance of the developed method is verified for various types of unknown input and disturbance. Furthermore, the performance of this method is compared with other unknown input estimation methods. The simulation results show better and acceptable performance of the demonstrated method rather than other input estimation methods. In spite of the benefits of the proposed method, its various free parameters and larger computation burden are the limitations of this method

Future recommendations

Here are some suggestions for improving the performance of the algorithm presented in this paper. Due to improved processor capabilities, it is now possible to use other geometric shapes like zonotopes instead of ellipsoidal sets. Therefore, it is suggested to use other convex sets for uncertainty modeling to improve the accuracy of the proposed exogenous input estimator performance. Another issue is the choice of the global optimal value of filter free parameters. Selecting the appropriate values for these parameters will have a significant impact on the performance of the UBB based estimators. It should be noted that the method presented in this paper calculates the sub-optimal values for the filter free parameters. Another suggestion is the design of robust UBB-based estimator for estimating the unknown input for the systems with the uncertain parameters of the dynamic system model.

References

1. Foo YK, Soh YC, Moayedi M (2012) Linear set-membership state estimation with unknown but bounded disturbances. Int J Syst Sci 43(4):715–730
2. Chui CK, Chen G (2017) Kalman filtering. Springer, Berlin
3. Fomin VN (2012) Optimal filtering: volume I: filtering of stochastic processes, vol 457. Springer, Berlin
4. Simon D (2006) The H∞ filter, in optimal state estimation. Wiley, Hoboken, pp 331–371
5. Schweppe FC (1973) Uncertain dynamic systems. Prentice-Hall, Upper Saddle River
6. Bertsekas D, Rhodes I (1971) Recursive state estimation for a set-membership description of uncertainty. IEEE Trans Autom Control 16(2):117–128
7. Schweppe F (1968) Recursive state estimation: unknown but bounded errors and system inputs. IEEE Trans Autom Control 13(1):22–28
8. Alamo T, Bravo JM, Camacho EF (2005) Guaranteed state estimation by zonotopes. Automatica 41(6):1035–1043
9. Chisci L, Garulli A, Zappa G (1996) Recursive state bounding by parallelotopes. Automatica 32(7):1049–1055
10. He L, Sun X (2010) Recursive triangulation description of the feasible parameter set for bounded-noise models. IET Control Theory Appl 4(6):985–992
11. Maksarov D, Norton J (1996) State bounding with ellipsoidal set description of the uncertainty. Int J Control 65(5):847–866
12. Gollamudi S et al (1996) Set-membership state estimation with optimal bounding ellipsoids. In: Proceedings of the international symposium on information theory and its applications
13. Scholte E, Campbell ME (2003) A nonlinear set-membership filter for on-line applications. Int J Robust Nonlinear Control 13(15):1337–1358
14. Wei G, Wang Z, Shen B (2010) Error-constrained filtering for a class of nonlinear time-varying delay systems with non-Gaussian noises. IEEE Trans Autom Control 55(12):2876–2882
15. Liu Y, Zhao Y, Wu F (2016) Ellipsoidal state-bounding-based set-membership estimation for linear system with unknown-but-bounded disturbances. IET Control Theory Appl 10(4):431–442
16. Ginoya D et al (2016) A new state and perturbation observer based sliding mode controller for uncertain systems. Int J Dyn Control 4(1):92–103
17. Guezmil A et al (2018) Unknown input observer-based active fault tolerant control for induction machine. Int J Dyn Control 6(2):726–738
18. Sharma V, Sharma BB, Nath R (2017) Unknown input reduced order observer based synchronization framework for class of nonlinear systems. Int J Dyn Control. https://doi.org/10.1007/s40435-017-0354-2

19. Khaloozadeh H, Karsaz A (2009) Modified input estimation technique for tracking manoeuvring targets. IET Radar Sonar Navig 3(1):30–41
20. Orjuela R et al (2009) On the simultaneous state and unknown input estimation of complex systems via a multiple model strategy. IET Control Theory Appl 3:877–890
21. Fang H, Shi Y, Yi J (2011) On stable simultaneous input and state estimation for discrete-time linear systems. Int J Adapt Control Signal Process 25(8):671–686
22. Shu H et al (2016) Unknown input and state estimation for linear discrete-time systems with missing measurements and correlated noises. Int J Gen Syst 45(5):648–661
23. Alirezapouri MA et al (2017) Unknown but bounded based input estimation method for maneuvering target tracking problem. In: Iranian conference on electrical engineering (ICEE), 2017. IEEE
24. Pope SB (2008) Algorithms for ellipsoids. Cornell University Report No. FDA, 08-01
25. Guderley K, Keller C (1971) Enclosing the vector sum of two ellipsoids with an ellipsoid. In: Abhandlungen aus dem Mathematischen Seminar der Universität Hamburg. Springer
26. Alirezapouri MA et al (2017) Set value observer performance improvement with optimizing the free parameter in the MTT problem. In: 36th Chinese control conference (CCC), 2017
27. Zhou B, Han J, Liu G (2008) A UD factorization-based nonlinear adaptive set-membership filter for ellipsoidal estimation. Int J Robust Nonlinear Control 18(16):1513–1531
28. Sontag ED (2008) Input to state stability: basic concepts and results. In: Nistri P, Stefani G (eds) Nonlinear and optimal control theory: lectures given at the C.I.M.E. Summer School held in Cetraro, Italy June 19–29, 2004. Springer, Berlin, pp 163–220
29. Anderson B, Moore JB (1981) Detectability and stabilizability of time-varying discrete-time linear systems. SIAM J Control Optim 19(1):20–32
30. Xie L, Soh YC, De Souza CE (1994) Robust Kalman filtering for uncertain discrete-time systems. IEEE Trans Autom Control 39(6):1310–1314
31. Krzemiński S, Kaczorek T (2004) Perfect reduced-order unknown-input observer for standard systems. Bull Pol Acad Sci 52:103–107
32. Hashemi E et al (2017) Real-time estimation of the road bank and grade angles with unknown input observers. Veh Syst Dyn 55(5):648–667
33. Ding B, Fang H (2017) Adaptive modified input and state estimation for linear discrete-time system with unknown inputs. Circuits Syst Signal Process 36(17):3630–3649